Canadian Mineralogist
Vol. 25, pp. 51-77 (1987)

THE RELATIONSHIP OF OLIVINE CUMULATES AND MINERALIZATION TO CYCLIC UNITS IN PART OF THE UPPER CRITICAL ZONE OF THE WESTERN BUSHVELD COMPLEX

ROGER N. SCOON AND WILLIAM J. DE KLERK
Department of Geology, Rhodes University, P.O. Box 94, Grahamstown 6140, South Africa

ABSTRACT

In the northern sector of the western Bushveld Complex, toward the top of the upper Critical Zone, magnesian olivine is an unusually abundant cumulus phase in the cyclic units between the UG-1 chromitite layer and the Bastard Reef. Field relationships, whole-rock chemistry and electron-microprobe analyses of olivine (Fo_{82-77}) from different cyclic units provide evidence that the chamber was intruded by new influxes of magma. The new influxes, intruding the chamber at the level of the UG-2 and Merensky Reefs, have not reached the "density-crossover point", thus intruding not as a jet or buoyant plume (Campbell *et al.* 1983), but as a flow along the crystal-liquid interface (Sparks & Huppert 1984). Cyclic units consisting entirely of ultramafic cumulates are attributed to fractional crystallization of a distinct stratified layer of new magma. The developing cyclic unit is then terminated by a further influx of magma. Hybrid cyclic units, however, consist of ultramafic cumulates sharply ovelain by felsic cumulates, and are attributed to the mixing of the new influx of magma with the column of supernatant liquid, the felsic cumulates having crystallized after the mixing event. From the association of Ni-rich olivine with Ni-rich sulfide we infer that some of the new influxes of magma that intruded the chamber between the UG-2 and Bastard Reefs reached saturation in S whilst olivine was still on the liquidus. The Ni/Fe ratio of the two phases is then controlled by the partition coefficient, $K_D^{Ni/Fe}$(sulf/oliv); for the Merensky Reef, we find $6 < K_D < 11$. Base-metal sulfide (BMS) and platinum-group element (PGE) mineralization occurs in ultramafic cumulates at the base of cyclic units, preferentially in cumulates with a pegmatoidal texture (*e.g.*, the Merensky Reef) and in certain chromitite layers (*e.g.*, the UG-2 Reef). We suggest that two stages of BMS mineralization occurred, namely cumulus and postcumulus; the PGE mineralization was related largely to a postcumulus event, involving upward-migrating intercumulus liquid.

Keywords: Bushveld Complex, cumulate, cyclic unit, Merensky Reef, magma mixing, magma influxes, nickel, olivine, platinum-group elements, South Africa, base-metal sulfides, UG-2 Reef, upper Critical Zone.

SOMMAIRE

Dans le secteur nord de la partie occidentale du complexe stratiforme du Bushveld, l'olivine magnésienne est anomalement abondante parmi les cumulats des unités cycliques situées entre le niveau de chromitite UG-1 et le récif Bastard. Les données du terrain, le chimisme des roches et la composition de l'olivine (Fo_{82-77}, par microsonde électronique) de différentes unités cycliques étayent l'hypothèse que la chambre magmatique a été envahie périodiquement par des venues de magma primaire. Ces venues, qui sont arrivées aux niveaux des unités UG-2 et du récif Merensky, n'avaient pas atteint le point d'égalité des densités, et avaient donc l'allure non pas d'un jet ou d'un panache (Campbell *et al.* 1983), mais plutôt de coulées le long de l'interface liquide-cumulats (Sparks et Huppert 1984). Les unités cycliques composées entièrement de cumulats ultramafiques résulteraient de la cristallisation fractionnée d'une couche distincte stratifiée de nouveau magma; le développement de l'unité cyclique se termine ensuite par la mise en place d'une nouvelle venue de magma. Toutefois, des unités cycliques hybrides, faites de cumulats ultramafiques en transition rapide à des cumulats felsiques, seraient le résultat d'un mélange du magma de la dernière venue au magma évolué surnageant, la formation des cumulats felsiques se plaçant après celle du mélange. L'association de l'olivine riche en nickel à une fraction de sulfure riche aussi en Ni fait penser que certaines des venues de magma primaire, qui sont arrivées dans la chambre entre les niveaux UG-2 et le récif Bastard, ont atteint la saturation en soufre lorsque l'olivine était encore sur le liquidus. Le rapport Ni/Fe des deux phases est alors fonction du coefficient de partage $K_D^{Ni/Fe}$(sulf/oliv). Le K_D pour le récif Merensky obéit à la relation $6 < K_D < 11$. La minéralisation en sulfures de métaux de base (BMS) et en éléments du groupe du platine (PGE) se trouve dans les cumulats ultramafiques, à la base des unités cycliques, surtout dans les cumulats de texture à tendance pegmatitique (par exemple, le récif Merensky) et dans certaines couches de chromitite (par exemple, le récif UG-2). Nous préconisons deux stades de minéralisation BMS: cumulus et post-cumulus; quant à la minéralisation PGE, elle serait surtout liée à un événement post-cumulus, marqué par la migration ascendante du liquide intercumulus.

(Traduit par la Rédaction)

Mots-clés: complexe du Bushveld, cumulats, unité cyclique, récif Merensky, mélange de magmas, incursions du magma, nickel, olivine, éléments du groupe du platine, Afrique du Sud, métaux de base, récif UG-2, zone critique supérieure.

INTRODUCTION

The appearance of plagioclase as a major cumulus phase was a significant event in the evolution of the layered sequence of the Busveld Complex. Cumulus plagioclase is absent in the Lower and lower

Critical Zones, where magnesian olivine, orthopyroxene and chromite are the dominant cumulus phases; in the upper Critical Zone, orthopyroxene and plagioclase are the major cumulus minerals, and chromite and magnesian olivine are subordinate. Above the upper Critical Zone, in the Main and Upper Zones, magnesian olivine and chromite are absent, and plagioclase, orthopyroxene, clinopyroxene, iron-rich olivine, Fe–Ti oxides and apatite are the principal cumulus phases. The upper Critical Zone is thus considered as transitional between the relatively primitive, ultramafic cumulates in the Lower and lower Critical Zones and the more fractionated, mafic–felsic cumulates in the Main and Upper Zones.

Magnesian olivine is rarely observed in the upper Critical Zone below the UG–1 chromitite layer, but is locally a significant cumulus phase toward the top of this zone, between the UG–1 chromitite layer and the Bastard Reef. The reappearance of magnesian olivine and the recurrence of major chromitite layers, after a thick sequence of orthopyroxene–plagioclase cumulates had crystallized [in the eastern Bushveld Complex, Cameron (1982) calculated that the upper Critical Zone below the UG–1 chromitite layer consists of 47.1 modal % orthopyroxene and 45.1 modal % plagioclase], must surely indicate that the chamber was replenished by new influxes of relatively primitive magma.

This study is based on two sections in the western Bushveld Complex, at the Amandelbult Section and Union Section mines of the Rustenburg Platinum Mines (RPM) group. The study sections are restricted to the sequence between the UG–1 chromitite layer and the Bastard Reef and lie wholly within the upper Critical Zone, as we position the base of the Main Zone at the top of the Bastard cyclic unit, rather than at the Merensky Reef as advocated by Willemse

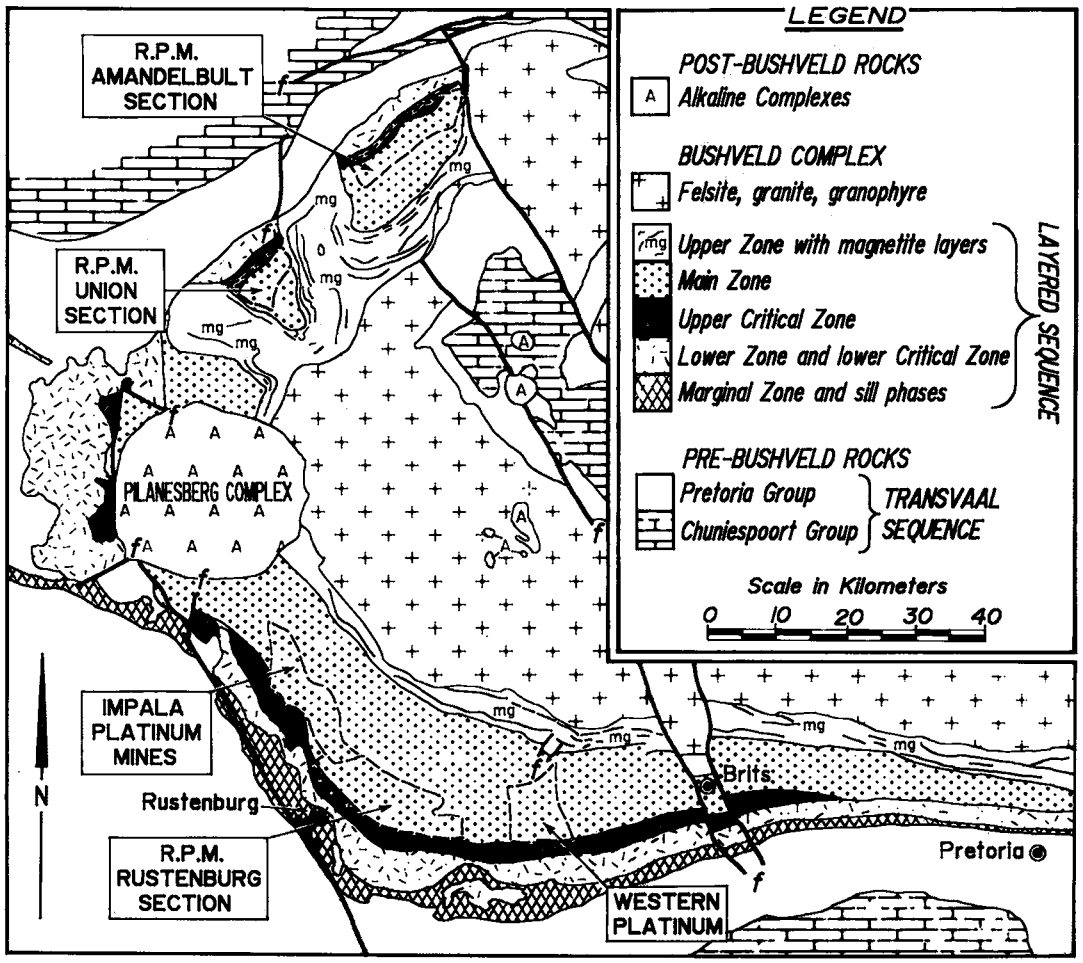

FIG. 1. Geology of the western Bushveld Complex. Dashed lines delimit the leaseholds of the principal platinum mines. R.P.M.: Rustenburg Platinum Mines.

(1969) and in many recent publications. The study sections are subdivided into cyclic units, designated wherever possible by their principal marker-layer; we apply the cumulate terminology of Wager *et al.* (1960) without genetic constraints, as recommended by Irvine (1982). Outcrop is very poor in these areas, and this study, which is directed toward olivine-bearing cumulates, is based on mapping and sampling of underground exposures and borehole core. New data from an electron-microprobe study of olivine and base-metal sulfides (BMS) are presented, together with whole-rock compositions of the olivine-bearing cumulates. The major platiniferous orebodies, the UG-2 and Merensky Reefs, occur in the study sections and, accordingly, the distribution of BMS and platinum-group-element (PGE) mineralization is discussed.

Field Relationships

Regional setting

The Amandelbult Section and Union Section mines are situated to the north of the Pilanesberg Complex, in the northern sector of the western Bushveld Complex (Fig. 1). In this area the Lower, Critical and Main Zones of the layered sequence crop out as two discrete segments, corresponding approximately to the leaseholds of the two mines. Cumulates in the Upper Zone conformably overlie the younger cumulates to the southeast, but transgress them to the southwest and in a structurally complex area between the two mines (colloquially referred to as the "Northern Gap"). The average dip of the layering is 20° southeast, but at the margins of the Northern Gap the layering swings round in an arc, eventually dipping at 50° or more to the southwest or northeast. Stratigraphic differences between cumulates in the Lower, Critical and Main Zones at the two mines may be attributed either to lateral changes along strike or to formation within entirely separate magma-chambers. Only minor lateral changes occur at the Union Section mine, but at the Amandelbult Section mine, where the upper Critical Zone is exposed in mine workings and borehole core for over 20 km along strike, considerable lateral variation is recognized (Fig. 2). For a detailed description of the upper Critical Zone above the UG-1 chromitite layer at these two mines, the reader is referred to Viljoen *et al.* (1986a, b).

Cyclic units

A cyclic unit may be described as a sequence of usually sharply defined cumulate layers that is repeated (more or less) in a systematic way (Jackson 1961, Irvine 1982). Within a cyclic unit the cumulate sequence typically appears to define the order in which minerals were fractionally crystallized from their parental magma (Irvine 1982). Cryptic mineralogical variations may occur, although they are not always present. Irvine (1982) observed that almost by definition cyclic units are incomplete. Cyclic units may develop owing to processes operating wholly within a magma chamber [*e.g.*, owing to classic cumulus processes as described by Wager *et al.* (1960) or resulting from bottom crystallization as envisaged by McBirney & Noyes (1979)], or they may be attributed to replenishment of the chamber by influxes of fresh magma, as described by many authors, including Brown (1956) and Irvine (1982). It is important to realize that the repetition of certain rock-types in a layered intrusive complex is based on field relations, but the definition of a cyclic unit is based on interpretation.

We recognize a minimum of seven cyclic units in the upper Critical Zone above the UG-1 chromitite layer at the Amandelbult Section and Union Section mines, namely the UG-1, UG-2, Lower Pseudoreef, Upper Pseudoreef, Footwall, Merensky and Bastard (Fig. 2). This subdivision follows the conventional approach of Jackson (1961, 1970) and Wager & Brown (1968), amongst others, and complies with field relationships and petrographic and chemical data. The UG-1, UG-2, Merensky and Bastard cyclic units are well known and may be correlated throughout the western sector of the Bushveld Complex (Feringa 1959, Wager & Brown 1968, Van Zyl 1970, Vermaak 1976). However, the Footwall cyclic unit exhibits considerable lateral variation and is difficult to correlate with the equivalent sequence in the Rustenburg area. The Lower Pseudoreef and Upper Pseudoreef cyclic units have only been described from the northern sector of the western Bushveld Complex; these latter three cyclic units are described below.

We suggest that all the cyclic units in the study sections commence with an ultramafic cumulate and that the most complete units, it is believed, are capped with anorthosite layers. Major chromitite layers are positioned at the base of cyclic units, although it is possible that olivine is locally the first liquidus phase. Very thin chromitite layers, or stringers, that may in part consist of reaction chromite as described by Lee *et al.* (1983), do not perforce signal the commencement of a new cyclic unit. Thus the sequence of crystallization of cumulus phases, from the base of a cyclic unit upward, is chromite, olivine (where present), orthopyroxene, plagioclase. A reasonably complete cyclic unit should exhibit the following sequence of cumulates with increasing height: chromitite, harzburgite, olivine orthopyroxenite, orthopyroxenite, melanorite, norite, leuconorite, anorthosite. However, it is significant that melanorite and norite are rare in the cyclic units in the study sections, particularly in the

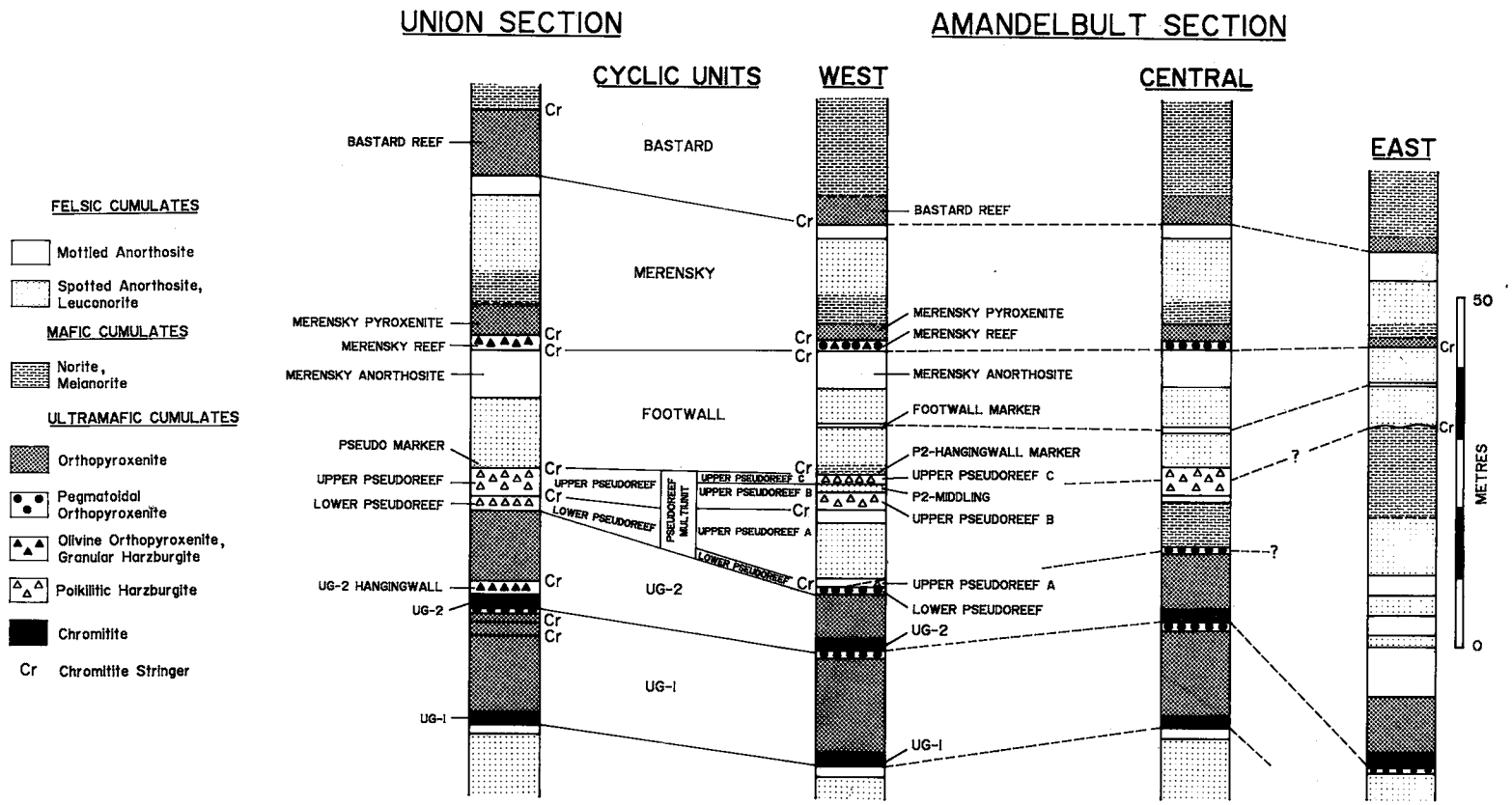

FIG. 2. Vertical columns of the study sections at the Amandelbult Section (west) and Union Section mines, showing correlation between the two mines and the lateral variation at the Amandelbult Section mine [columns for central and eastern parts of the mine from Viljoen *et al.* (1986b)].

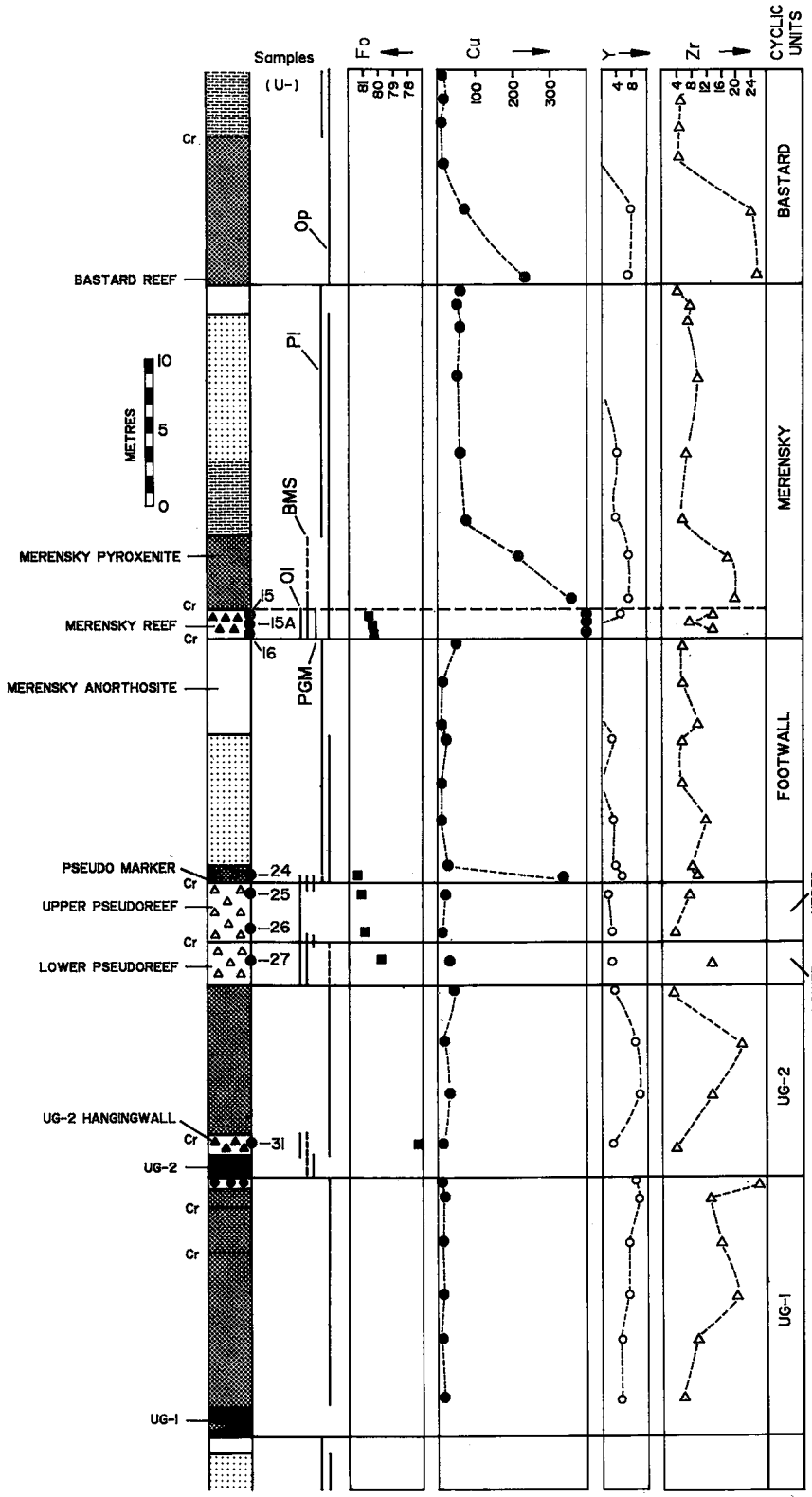

FIG. 3. Details of the study at the Union Section mine showing sampling positions (U-26, *etc.*) and distribution of cumulus olivine (Ol), cumulus orthopyroxene (Op), cumulus plagioclase (Pl), base-metal sulfides (BMS) and platinum-group minerals (PGM). Composition of olivine in mol. % Fo, and distribution of Cu, Y and Zr from whole-rock data in ppm. For explanation of rock types, see Figure 2.

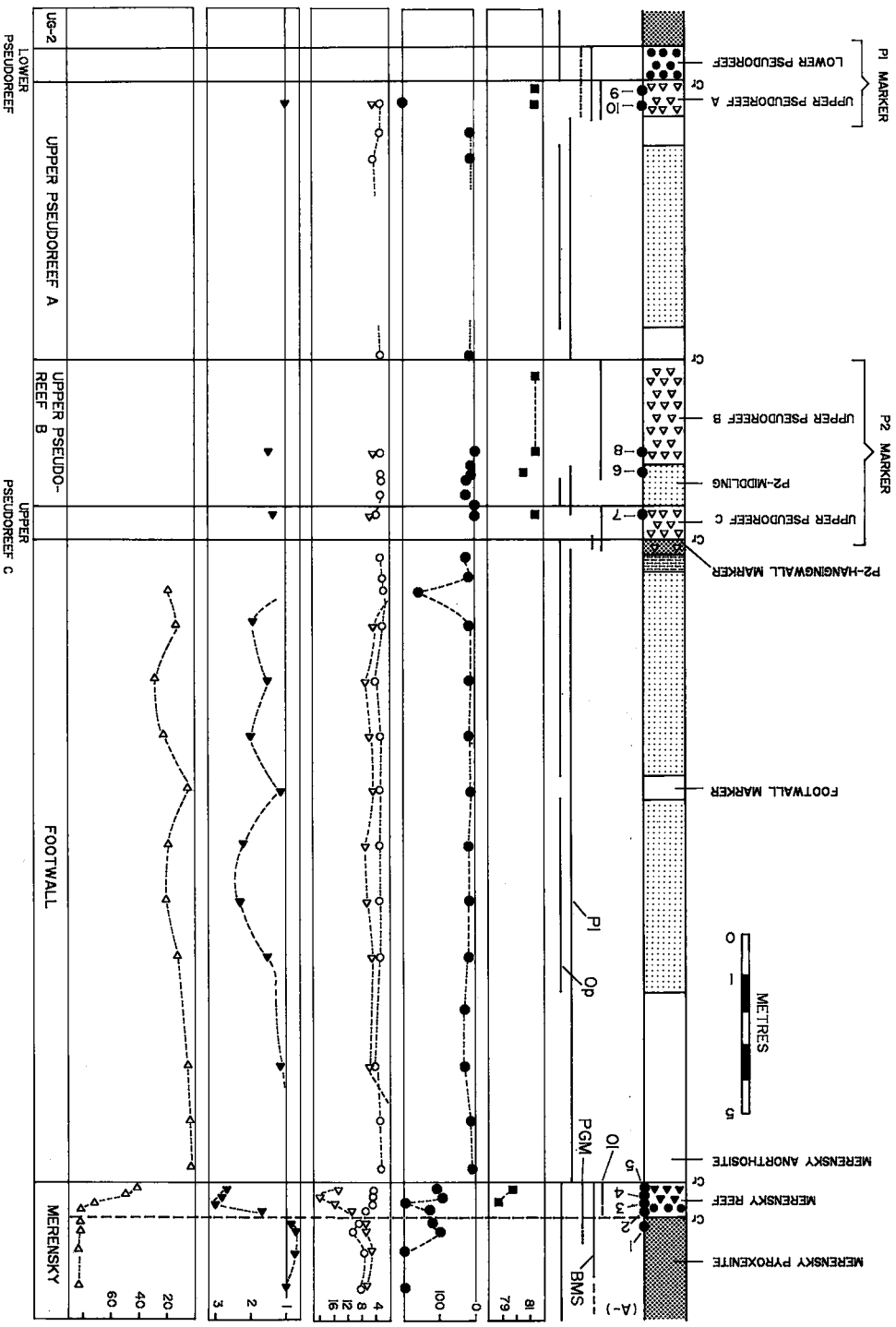

FIG. 4. Details of the study section at the Amandelbult Section mine showing sampling positions (A–7, *etc.*) and distribution of cumulus olivine (Ol), cumulus orthopyroxene (Op), cumulus plagioclase (Pl), base-metal sulfides (BMS) and platinum-group minerals (PGM). Composition of olivine in mol. % Fo, distribution of Cu, Y and Zr from whole-rock data in ppm, and normative pyroxene from the CIPW norm. For explanation of rock types, see Figure 2.

cyclic units below the Merensky Reef. Because of this observation we categorize the cumulates in our study into three groups, "ultramafic" (chromitite, harzburgite, olivine orthopyroxenite, orthopyroxenite), "mafic" (melanorite, norite) and "felsic" (leuconorite, anorthosite). Moreover, we also recognize three types of cyclic units, *i.e.*, (1) those consisting entirely of ultramafic cumulates (*e.g.*, the UG-1, UG-2 and Lower Pseudoreef cyclic units); (2) those consisting of ultramafic cumulates that are sharply overlain by felsic cumulates (*e.g.*, the Upper Pseudoreef A and B and Footwall cyclic units). This type of cyclic unit is interpreted as a hybrid and cannot be explained by a simple fractional-crystallization model operating wholly within the chamber; and (3) those consisting of a gradational sequence of ultramafic–mafic–felsic cumulates that may possibly be attributed to fractional crystallization from one magma (*e.g.*, the Merensky and Bastard cyclic units).

Because of the significance that is now placed on anorthosite cumulates in the formation of cyclic units, it is pertinent to realize that two principal varieties are recognized: spotted and mottled. Spotted anorthosite consists of cumulus plagioclase (over 90 modal %) and cumulus orthopyroxene, and may be considered as the felsic end-member resulting from cotectic crystallization of orthopyroxene and plagioclase. In mottled anorthosite (the mottled or poikilophitic texture is attributable to oikocrysts of orthopyroxene, clinopyroxene, or, more rarely, olivine); plagioclase (which usually, but not always, represents over 90 modal %) is the only demonstrably cumulus phase. The formation of mottled anorthosite is contentious; for example, Vermaak (1976) and Eales (1987) suggested that anorthosite mats float above new influxes of denser magma, whereas Todd *et al.* (1982) and Irvine *et al.* (1983) advocated that they are derivatives of a separate liquid (and, consequently, that anorthosite layers may occur at the base of cyclic units, not at the top). Because of this controversy, it is inappropriate to categorize new cyclic units entirely on the basis of anorthosite layers.

The Lower Pseudoreef cyclic unit

The "Pseudoreef" at the Union Section mine, as defined by Wager & Brown (1968), comprises the Lower Pseudoreef, a thin (1 cm thick) chromitite layer and the Upper Pseudoreef (Figs. 2, 3). We define the Lower Pseudoreef cyclic unit as comprising only the Lower Pseudoreef, a pegmatoidal, feldspathic harzburgite. The sequence between the UG-2 and Footwall cyclic units at the Amandelbult Sec-

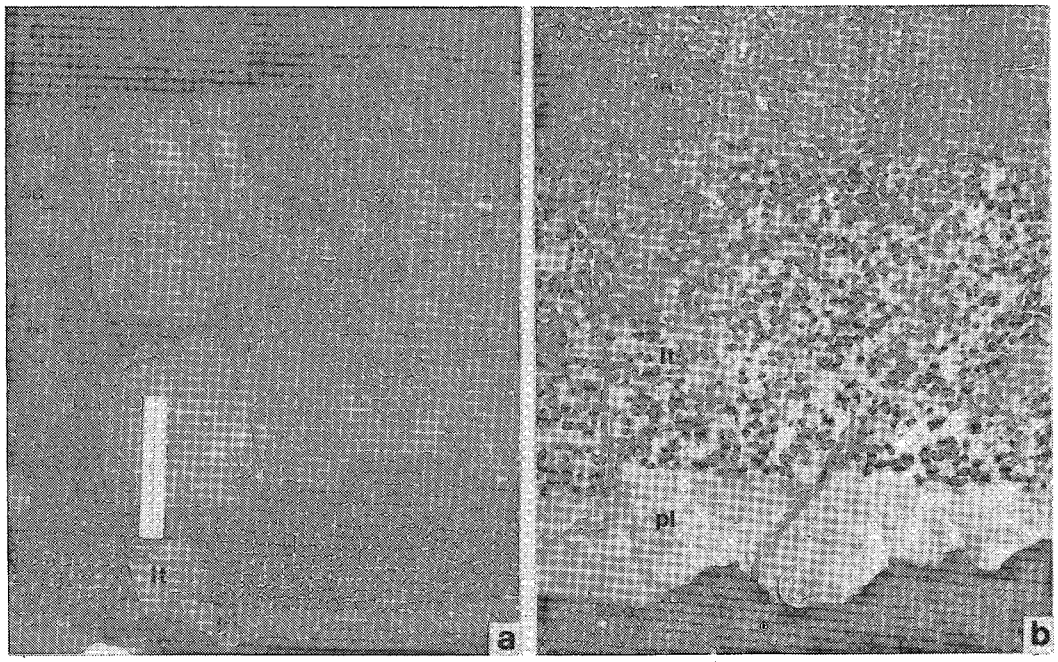

FIG. 5. (a) The P2 middling at the Amandelbult Section mine enclosed between two harzburgite layers, the Upper Pseudoreefs B (b) and C (c). The P2 middling consists of a well-defined layer of mottled anorthosite or leucotroctolite (lt) and a layer of leuconorite (ln) that grades upward into spotted anorthosite (sa). Scale: 30 cm. (b) The base of the P2 middling illustrating the layer of plagioclase (pl) between the harzburgite and the leucotroctolite layer and the scalloped contact.

tion mine is rather complex and is referred to by us as the "Pseudoreef multiunit"; it exhibits considerable variation along strike and may comprise four cyclic units (Fig. 2). The Lower Pseudoreef cyclic unit at this mine is defined as the layer of pegmatoidal, feldspathic orthopyroxenite that directly overlies the UG–2 cyclic unit. It is equated with the basal portion of the Lower Pseudoreef (or "P1 marker") of Viljoen *et al.* (1986b; see Fig. 4).

We recognize the Lower Pseudoreef as a separate cyclic unit for the following reasons. Firstly, the Lower Pseudoreef at the Union Section mine has a lower olivine:orthopyroxene ratio than the Upper Pseudoreef, and at the Amandelbult Section mine olivine is absent in (our definition of) the Lower Pseudoreef. Secondly, a laterally persistent chromitite layer separates the two pseudoreefs. Thirdly, the Lower and Upper Pseudoreefs are mineralogically quite distinct, and olivine in the Lower Pseudoreef is more fractionated (see below).

The Upper Pseudoreef cyclic unit(s)

The Upper Pseudoreef cyclic unit at the Union Section mine consists of a basal layer of chromitite and a coarse- to medium-grained, feldspathic harzburgite (the Upper Pseudoreef), colloquially described as the "tarentaal", because its distinctive spotted appearance resemble the markings of the guinea fowl, or tarentaal. This part of the Pseudoreef multiunit at the Amandelbult Section mine is divided into three cyclic units, the Upper Pseudoreefs A, B and C (Fig. 4). Unit A consists of a basal layer of chromitite (1 cm thick), a discontinuous layer of coarse-grained, feldspathic harzburgite (with a maximum thickness of 0.5 m; the Upper Pseudoreef A), and a composite package of felsic cumulates (5 – 6 m thick) that comprise layers of mottled anorthosite at the base and top, separated by a layer of leuconorite. Unit B consists of a basal chromitite layer (0.5 – 1 cm thick), a layer of feldspathic harzburgite (approximately 3 m thick; the Upper Pseudoreef B), and a composite package of felsic cumulates (1 – 1.2 m thick), colloquially described as the "P2 middling". The P2 middling consists of a basal layer of mottled anorthosite or leucotroctolite (the oikocrysts are olivine, an unusual feature) that is sharply overlain by a layer of leuconorite that itself is transitional upward into spotted anorthosite (Fig. 5). Unit C comprises only a layer of feldspathic harzburgite (approximately 1 m thick; the Upper Pseudoreef C). The Upper Pseudoreef A forms the upper part of the P1 marker, and the Upper Pseudoreefs B and C form the "P2 marker" of Viljoen *et al.* (1986b) (Fig. 4). The Upper Pseudoreefs A, B and C are mineralogically compared with the tarentaal, and may be correlated with the Upper Pseudoreef at the Union Section mine.

The Footwall cyclic unit

The Footwall cyclic unit at the Union Section mine consists of a basal chromitite layer (1 cm thick) and a thin layer (20 cm thick) of pegmatoidal, feldspathic harzburgite (the "Pseudo marker") that is transitional upward over 1 – 2 m through layers of medium-grained olivine orthopyroxenite, melanorite and norite into a composite package of felsic cumulates. These latter comprise a sequence of leuconorites and spotted anorthosites capped by a well-defined layer of mottled anorthosite [the "Merensky (footwall) anorthosite"]. Approximately 0.5 m above the base of the unit is a thin (1 – 2 cm), yet persistent layer of mottled anorthosite (the "Pothole marker").

The Footwall cyclic unit at the Amandelbult Section mine commences with a chromitite layer (1 cm thick) that is overlain by a layer of pegmatoidal, feldspathic harzburgite (10 – 15 cm thick). This harzburgite layer is transitional upward over approximately 0.5 – 1 m into a melanorite–norite layer, which itself rapidly grades upward into a thick layer of leuconorite that is capped by a well-defined layer of mottled anorthosite [the "Merensky (footwall) anorthosite"]. Within the melanorite–norite layer, approximately 0.7 m above the base of the unit, is a thin layer (1 – 1.5 cm thick) of anorthosite (the "P2 hangingwall marker"), that is correlated with the "Pothole marker" at the Union Section mine. A laterally continuous layer (1 m thick) of mottled anorthosite (the "Footwall marker") occurs in the leuconorite layer approximately 10 m below the Merensky Reef. This anorthosite layer may be correlated with the equivalent layer at the Rustenburg Section mine of RPM (Fig. 1), but is absent at the Union Section mine. Apart from the Footwall marker, the Footwall cyclic unit at both the Amandelbult Section and Union Section mines is very similar.

Lateral variation and scalloped contacts

Lateral variation of both discrete layers and cyclic units is prevalent in the upper Critical Zone at the Amandelbult Section mine (Fig. 2), as described by Viljoen *et al.* (1986b). Vermaak (1976) discussed lateral variation within the cyclic units in the western Bushveld Complex, and suggested that the Merensky Reef unconformably overlies the (Merensky) Footwall cyclic unit. Kruger & Marsh (1982, 1985) argued that this unconformity is related to resorption of the cumulate pile immediately below the crystal–liquid interface (see also Irvine *et al.* 1983). Lateral variation at the Amandelbult Section mine is restricted largely to ultramafic cumulate layers, and does not occur in layers at the top of cyclic units, as would be expected if attributable to resorption. For example, the harzburgite layers in the Pseudoreef

multiunit exhibit considerable lateral variation, whereas delicately layered anorthosite markers are laterally very persistent.

Many of the ultramafic layers in the study sections display scalloped (dimpled) contacts, particularly where they occur adjacent to layers of mottled anorthosite, *e.g.*, the footwall to the Merensky Reef and the lower and upper contacts of some of the harz-

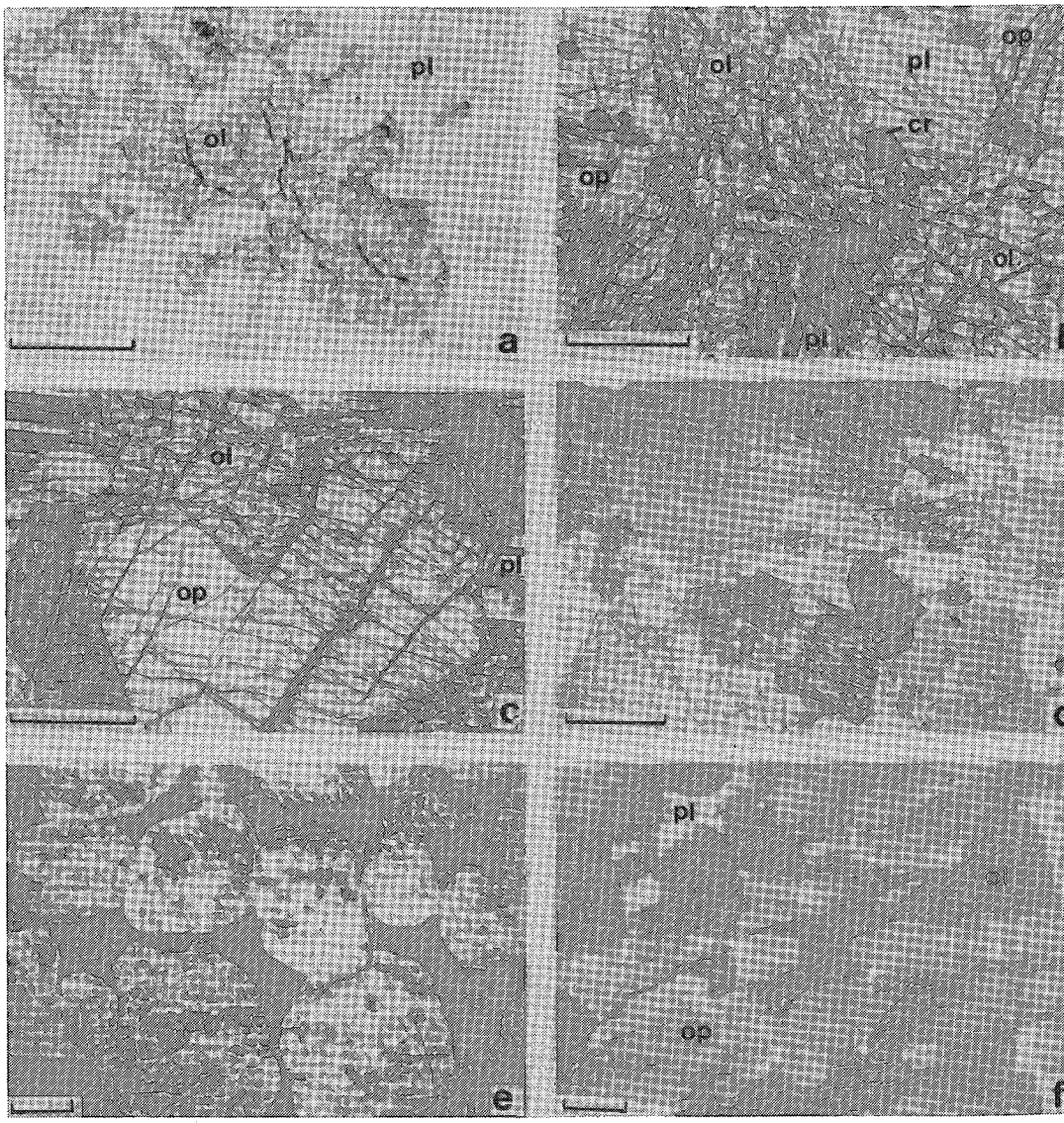

FIG. 6. (a) Olivine oikocrysts enclosing cumulus plagioclase. Plagioclase not enclosed by olivine is well annealed. Leucotroctolite (sample A–6). (b) Sharp contacts between cumulus olivine + orthopyroxene and intercumulus plagioclase; where plagioclase is absent, reaction replacement results in a xenomorphic texture. Chromite is absent from the olivine grains. (c) Subhedral orthopyroxene moulded around enhedral olivine, both enclosed by intercumulus plagioclase. (d) Mosaic of orthopyroxene grains exhibiting a xenomorphic texture. (b), (c), (d) are all from the same thin section. Feldspathic (granular) harzburgite (sample U–31). (e) Cumulus olivine (partially serpentinized) enclosed by intercumulus orthopyroxene. Feldspathic (poikilitic) harzburgite or tarentaal (sample U–26). (f) Large oikocryst of orthopyroxene enclosing cumulus olivine with minor intercumulus plagioclase. Olivine adjacent to plagioclase is subhedral, that adjacent to orthopyroxene is anhedral, a result of reaction replacement. Feldspathic (poikilitic) harzburgite or tarentaal (sample A–8). Abbreviations: olivine ol, orthopyroxene, op, plagioclase pl, chromite cr. Scale bar: 1 mm (a,b,c) and 2 mm (d,e,f,). (a) plane-polarized transmitted light, (b,c,d,e) crossed polarizers, transmitted light, (f) plane-polarized reflected light.

burgite layers in the Pseudoreef multiunit (Fig. 5b). These features may be similar, although less well developed, to the finger structures described from the Rhum Complex by Butcher *et al.* (1985). Some scalloped contacts may be attributed to resorption, but the scalloped upper contacts of harzburgite layers are probably best explained as postcumulus features.

Petrography and Chemistry of the Olivine-Bearing Cumulates

Sampling and analytical details

In the study section at the Union Section mine (Fig. 3), cumulus olivine occurs in an ultramafic cumulate above the UG-2 chromitite layer (the "UG-2 hangingwall"; sample U-31), the Lower Pseudoreef (sample U-27), the Upper Pseudoreef (samples U-25,26), the Pseudo marker (sample U-24) and the Merensky Reef (samples U-15,15A, 16). In the study section at the Amandelbult Section mine (Fig. 4), cumulus olivine occurs in the Upper Pseudoreef A (samples A-9,10), the Upper Pseudoreef B (sample A-8), the Upper Pseudoreef C (sample A-7), a harzburgite layer at the base of the Footwall cyclic unit (not sampled) and the Merensky Reef (samples A-2,3,4,5). Olivine occurs as oikocrysts in a leucotroctolite layer in the P2 middling (sample A-6; Fig. 6a). Wager & Brown (1968) reported olivine in the Bastard Reef at the Union Section mine, but this has not been sampled.

Whole-rock samples were analyzed for major elements by X-ray fluorescence on a Philips PW-1410 spectrometer, according to the method of Norrish & Hutton (1969). Sodium and selected trace elements were determined on powder briquettes. Full corrections were applied for spectral line and background interferences, dead-time and instrument drift. CIPW norms were calculated using a program based on the algorithm of Kelsey (1965). The percentage of Fe^{3+} has been estimated assuming a constant Fe_2O_3/FeO ratio of 0.1. Electron-microprobe data of olivine reported here were determined using a Cambridge Microscan unit, operating at 20 kV. Count rates were corrected using the routine of Bence & Albee (1968). All the above analytical work was completed in the Department of Geology, Rhodes University. Electron-microprobe analysis of BMS was carried out at the laboratories of the Johannesburg Consolidated Investment Company.

Petrography

Jackson (1961) made an important distinction between granular and poikilitic harzburgite in the Stillwater Complex, based on the textural relationships of olivine and orthopyroxene, and independent of the nature of the intercumulus phases. In all of

TABLE 1. WHOLE-ROCK COMPOSITIONS OF OLIVINE-BEARING CUMULATES*

	U-15	U-15A	U-16	U-24	U-25	U-27	U-31	A-1	A-2	A-3	A-4	A-5	A-6	A-7	A-8	A-9	A-10
wt.%																	
SiO_2	44.10	40.50	42.10	50.20	40.70	45.00	46.10	53.00	52.66	50.83	50.88	46.67	45.22	38.46	39.25	39.93	37.94
TiO_2	0.14	0.15	0.15	0.18	0.09	0.14	0.13	0.24	0.36	0.17	0.17	0.15	0.06	0.11	0.19	0.10	0.16
Al_2O_3	6.62	4.56	4.10	5.16	4.00	6.50	4.90	5.31	4.67	5.57	11.65	9.11	26.11	3.21	4.31	3.86	5.67
Fe_2O_3	1.12	1.49	1.30	0.97	1.10	1.10	1.20	1.05	1.11	1.07	0.86	1.02	0.31	1.81	1.16	1.31	1.22
FeO	11.15	14.94	13.04	9.74	10.98	10.98	11.97	10.55	11.05	10.70	8.59	10.23	3.10	11.77	11.59	13.12	12.18
MnO	0.20	0.19	0.19	0.22	0.23	0.17	0.24	0.29	0.22	0.18	0.13	0.20	0.03	0.15	0.15	0.18	0.19
MgO	25.40	27.60	28.10	26.00	32.20	27.50	28.70	23.12	24.23	24.02	19.21	22.90	7.31	31.03	31.06	30.01	28.91
CaO	3.66	2.28	2.62	3.67	2.23	3.70	3.40	4.89	3.65	3.61	5.38	4.28	12.63	2.87	2.39	2.24	2.35
Na_2O	0.60	0.40	0.40	0.50	0.40	0.60	0.60	0.43	0.43	0.50	0.91	0.58	1.78	0.11	0.13	0.13	0.26
K_2O	0.09	0.11	0.09	0.04	0.07	0.11	0.05	0.03	0.19	0.15	0.78	0.64	0.23	0.06	0.06	0.03	0.03
P_2O_5	n.d.	n.d.	n.d.	n.d.	0.01	0.02	0.01	0.01	0.02	0.01	0.02	0.01	0.01	n.d.	n.d.	n.d.	n.d.
Cr_2O_3	0.58	0.51	0.51	0.59	0.16	0.42	0.53	0.52	0.60	0.57	0.18	0.36	0.12	0.18	0.17	0.18	1.99
NiO	0.32	0.39	0.60	0.25	0.26	0.20	0.18	0.11	0.12	0.36	0.15	0.20	0.05	0.26	0.25	0.33	0.36
L.O.I.	5.77	6.40	7.02	2.80	7.10	4.95	2.50	1.06	1.41	2.04	1.20	4.22	3.31	10.91	10.45	8.57	8.36
TOTAL	99.75	99.52	100.22	100.32	99.53	101.39	100.51	100.61	100.72	99.78	100.21	100.57	100.27	100.30	101.15	99.99	99.62
ppm																	
Cu	400	600	1100	400	19	37	10	216	130	820	99	111	15	8	10	386	504
Co	143	201	182	118	145	93	142	101	105	130	100	125	42	146	152	166	169
V	74	58	68	106	39	56	86	168	133	108	44	53	12	51	41	41	45
Sc	-	-	-	-	-	-	-	36	25	20	4	9	4	10	8	11	9
Sr	80	72	58	70	58	88	73	63	49	65	145	109	412	54	60	53	61
Rb	4	3	4	n.d.	3	3	n.d.	n.d.	6	5	28	29	4	n.d.	3	n.d.	n.d.
Zr	14	8	14	10	8	14	4	8	11	16	85	15	n.d.	6	5	4	3
Y	5	n.d.	n.d.	5	2	3	3	9	7	6	5	6	3	5	4	4	n.d.
CIPW wt.% norm																	
Ol	37.3	56.1	49.7	15.2	63.1	41.5	41.0	-	3.6	9.7	10.7	27.9	16.8	65.5	62.3	56.9	58.5
Op	35.2	24.2	29.9	60.3	19.2	31.9	34.8	70.7	72.5	65.8	48.6	39.4	0.9	16.7	21.1	26.7	19.7
Cp	2.6	0.9	3.3	5.3	1.8	2.9	5.1	9.4	6.2	4.5	0.9	0.6	-	5.5	0.8	1.1	-
Pl	22.1	15.4	14.0	16.6	13.8	21.2	16.2	16.6	15.2	18.2	38.2	30.3	81.6	10.5	13.8	12.2	15.4
Mg-No.	.80	.77	.79	.83	.84	.82	.81	.80	.80	.80	.80	.80	.81	.82	.83	.80	.81

n.d. : not determined; Mg-No : at.% $Mg/(Mg+Fe^{2+})$.
CIPW norms Ol : olivine; Op : orthopyroxene; Cp : clinopyroxene; Pl : plagioclase.
UNION SECTION U-15,15A,16 : Merensky Reef; U-24 : Pseudo marker; U-25 : Upper Pseudoreef; U-27 : Lower Pseudoreef; U-31 : UG-2 Hangingwall.
AMANDELBULT SECTION A-1 : Merensky pyroxenite; A-2,3,4,5 : Merensky Reef; A-6 : "P2 middling" (leucotroctolite); A-7 : Upper Pseudoreef C; A-8 : Upper Pseudoreef B; A-9,10 : Upper Pseudoreef A.
* Determined by X-ray-fluorescence analysis.

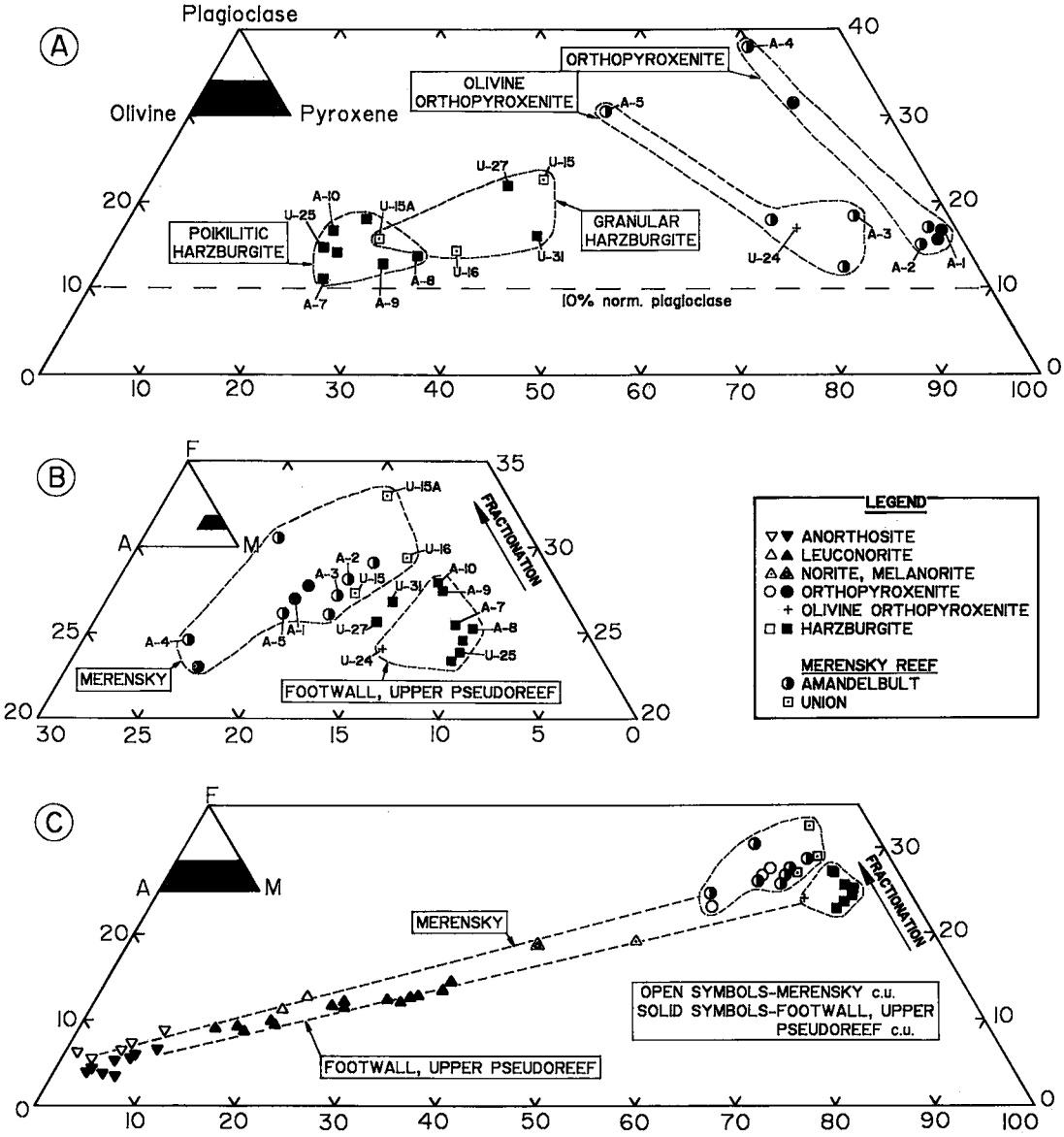

FIG. 7. (A) Part of a triangular plot of normative olivine–plagioclase–pyroxene. Each symbol represents the CIPW norm of one whole-rock composition. (B,C) Parts of a modified AFM diagram where A = wt.% ($CaO + Na_2O + K_2O$), F = wt.% FeO, M = wt.% MgO. Each symbol represents one whole-rock composition; (B) comprises only ultramafic cumulates, and (C) includes felsic cumulates.

the ultramafic cumulates in the study sections intercumulus plagioclase amounts to more than 10 modal %; hence in accordance with the practice of other Bushveld investigators the modifier "feldspathic" is applied. The modal mineralogy of the rocks discussed below may be simulated by the CIPW norm (Table 1; see also Fig. 7A).

Poikilitic harzburgites

The Upper Pseudoreefs (samples U-25,26 and A-7,8,9,10) at both mines are coarse- to medium-grained feldspathic (poikilitic) harzburgites that typically consist of cumulus olivine (60 – 70 modal %), cumulus chromite (0.5 – 1.5 modal %), intercumu-

lus orthopyroxene (10 – 25 modal %) and intercumulus plagioclase (10 – 15 modal %). Accessory phases include biotite (relatively common), amphibole and clinopyroxene. Much of the olivine is serpentinized, and secondary magnetite is abundant. The olivine occurs as large (5 – 10 mm) anhedral grains and also as small (less than 1 mm) euhedral to subhedral grains, the latter enclosed by plagioclase. The large olivine grains mutually embay and define a xenomorphic texture. Orthopyroxene occurs as large (up to 30 mm) oikocrysts enclosing olivine and as small (less than 1 mm) euhedral to subhedral grains, the latter enclosed in plagioclase. Olivine enclosed in orthopyroxene is considered as relict, apparently because of reaction replacement (Figs. 6e,f). Primary growth of olivine was apparently arrested by both reaction replacement (to form orthopyroxene) and by crystallization of plagioclase in the available intercumulus sites.

Granular harzburgites and olivine orthopyroxenites

Granular harzburgites and olivine orthopyroxenites in the study section are texturally comparable, differing only in the relative proportion of olivine and orthopyroxene. These comprise the UG–2 hangingwall (sample U–31), the Lower Pseudoreef (sample U–27), the Pseudo marker (sample U–24) and the Merensky Reef (samples U–15,15A,16 and A–2,3,4,5) (Fig. 8). The UG–2 hangingwall is a pegmatoidal, feldspathic (granular) harzburgite that consists of cumulus olivine (35 – 45 modal %), cumulus chromite (0.5 – 1.0 modal %), cumulus and intercumulus orthopyroxene (30 – 40 modal %) and intercumulus plagioclase (10 – 20 modal %). Accessory clinopyroxene (often as large oikocrysts) and biotite occur. Monomineralic aggregates of both olivine and orthopyroxene exhibit a xenomorphic texture (Fig. 6d), and reaction replacement of olivine by orthopyroxene is common. Small euhedral to subhedral grains of olivine and orthopyroxene occur enclosed in plagioclase, and the latter may be moulded around olivine (Fig. 6c). Distinctive features are the abundance of chromite adjacent to olivine grains and the paucity of chromite within olivine

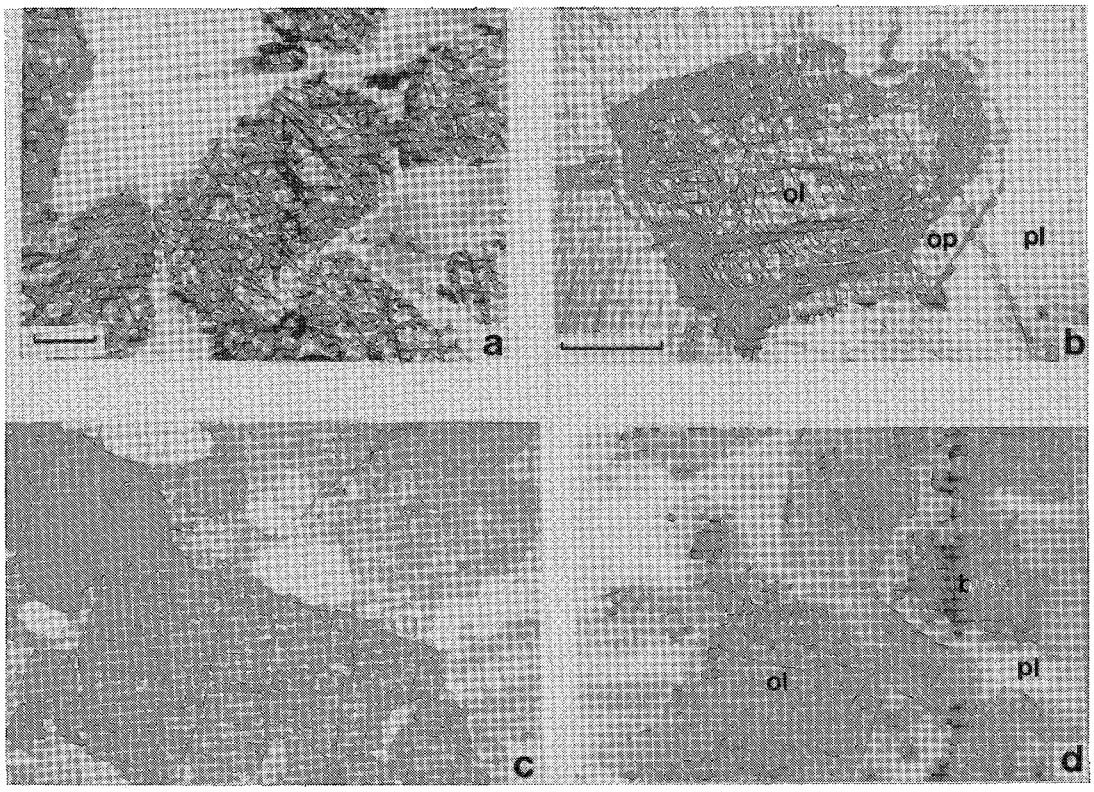

FIG. 8. (a) Cumulus olivine grains enclosed by intercumulus plagioclase. Base of Merensky Reef (sample U–16). (b) Olivine grain rimmed and partly replaced by orthopyroxene, both enclosed by intercumulus plagioclase. Merensky Reef (sample A–4). (c) Mosaic of orthopyroxene grains exhibiting a xenomorphic texture. Top of Merensky Reef (sample A–2). (d) Cumulus olivine and cumulus (?) base-metal sulfide grain (bms) enclosed by intercumulus plagioclase. Merensky Reef (sample A–3). Scale bar: 2 mm. (a,d) plane-polarized reflected light, (b,c) crossed polarizers, transmitted light. Scale in c and d is the same as in a.

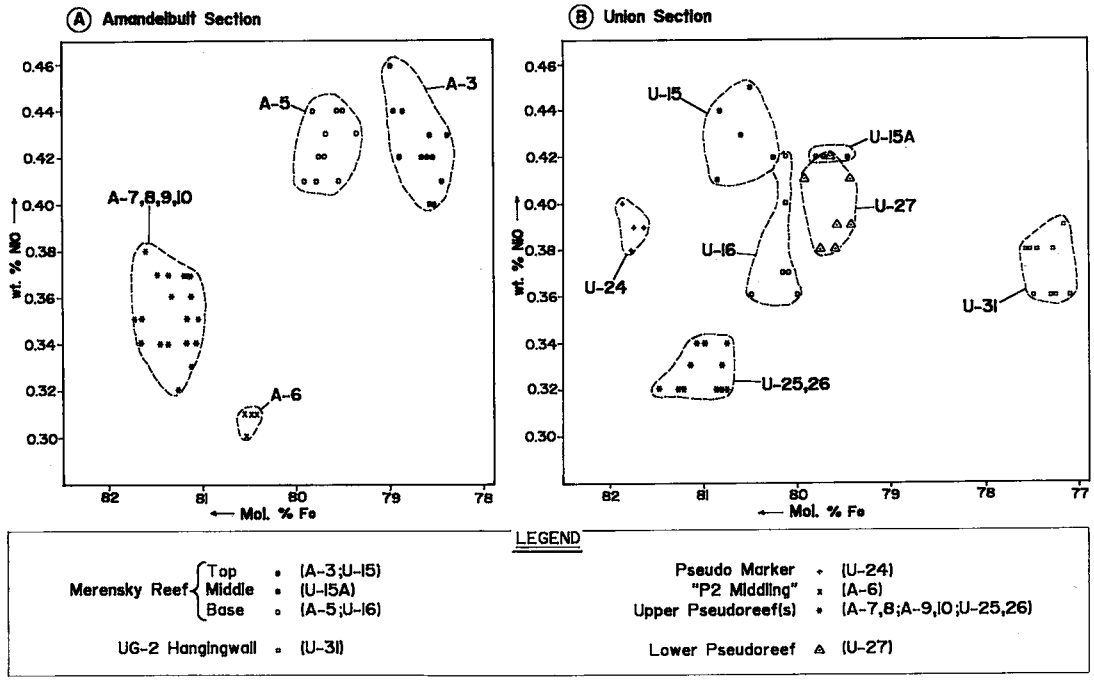

FIG. 9. Plot of wt.% NiO against mol.% Fo in olivine. Each symbol represents one analysis by electron microprobe.

TABLE 2. CHEMICAL COMPOSITION OF OLIVINE*

	U-15	U-15A	U-16	U-24	U-25/26	U-27	U-31	A-3	A-5	A-7/8	A-9/10	A-6
wt.%												
SiO_2	39.56	39.25	39.58	38.86	39.56	39.13	38.75	38.80	39.10	39.28	39.35	38.75
FeO	17.85	18.91	18.31	17.03	18.08	18.82	21.04	19.69	18.93	17.50	17.25	18.14
MnO	0.22	-	0.24	0.23	0.22	0.23	0.26	0.25	0.22	0.23	0.23	0.24
MgO	42.17	41.88	41.36	43.13	42.83	41.22	39.76	40.45	41.34	42.44	42.33	41.96
CaO	0.03	-	0.03	0.01	0.02	0.02	0.03	0.02	0.01	0.02	0.02	0.10
NiO	0.44	0.42	0.37	0.40	0.32	0.38	0.36	0.42	0.41	0.37	0.34	0.31
TOTAL	100.27	100.46	99.89	99.66	101.03	99.80	100.20	99.63	100.01	99.84	99.52	99.50
cations												
Si	1.0049	.9996	1.0107	.9915	.9981	1.0036	1.0007	1.0018	1.0015	1.0009	1.0045	.9951
Fe^{2+}	.3792	.4028	.3910	.3634	.3815	.4037	.4544	.4252	.4055	.3730	.3683	.3896
Mn	.0047	-	.0052	.0050	.0047	.0050	.0057	.0055	.0048	.0050	.0050	.0052
Mg	1.5964	1.5895	1.5740	1.6401	1.6105	1.5756	1.5302	1.5565	1.5780	1.6118	1.6103	1.6059
Ca	.0008	-	.0008	.0003	.0005	.0005	.0008	.0006	.0003	.0006	.0005	.0028
Ni	.0090	.0086	.0076	.0082	.0065	.0079	.0075	.0088	.0085	.0078	.0070	.0064
TOTAL	2.9950	3.0005	2.9893	3.0085	3.0018	2.9963	2.9993	2.9984	2.9986	2.9991	2.9956	3.0050
mol.% Fo	80.81	79.78	80.10	81.86	80.85	79.60	77.10	78.54	79.56	81.21	81.39	80.48
n	5	3	6	4	11	7	9	12	10	11	7	4
Fo x	80.61	79.65	80.17	81.76	81.02	79.61	77.33	78.68	79.66	81.31	81.37	80.51
Fo s	.2473	.1665	.1670	.0821	.2473	.1778	.1576	.2232	.1612	.2621	.1746	.0222
NiO x	0.43	0.42	0.38	0.39	0.33	0.40	0.37	0.42	0.425	0.36	0.35	0.31
NiO s	.0158	-	.0245	.0082	.0009	.0160	.0107	.0173	.0127	.0143	.0198	.0050

n : number of samples; x : mean; s : standard deviation; n.d. : not determined.
UNION SECTION U-15,15A,16 : Merensky Reef; U-24 : Pseudo marker; U-25,26 : Upper Pseudoreef; U-27 : Lower Pseudoreef; U-31 : UG-2 Hangingwall.
AMANDELBULT SECTION A-3,5 : Merensky Reef; A-7,8 : Upper Pseudoreef B,C; A-9,10 : Upper Pseudoreef A; A-6 : Oikocrysts from the "P2 middling" (leucotroctolite).
* Determined by electron-microprobe analysis.

grains (in contrast to the situation in the poikilitic varieties; Fig. 6b).

The Merensky Reef (defined as the pegmatoidal portion of the platiniferous orebody that occurs near the base of the Merensky cyclic unit) at both mines is enclosed by an upper and lower chromitite layer. At the Union Section mine the reef is unusually olivine-rich and varies from a feldspathic (granular) harzburgite to a feldspathic olivine orthopyroxenite; it has been described by Wager & Brown (1968), Van Zyl (1970) and Viljoen *et al.* (1986a). The reef at the Amandelbult Section mine, as described by Viljoen *et al.* (1986b), is a feldspathic olivine orthopyroxenite or feldspathic orthopyroxenite in which olivine is an accessory phase. The base of the reef may be relatively olivine-rich. The Merensky Reef is characterized by an exceptionally coarse-grained texture, by the presence of olivine, by abundant hydrous accessory phases such as mica and amphibole, and exotic phases such as zircon, graphite and quartz (an

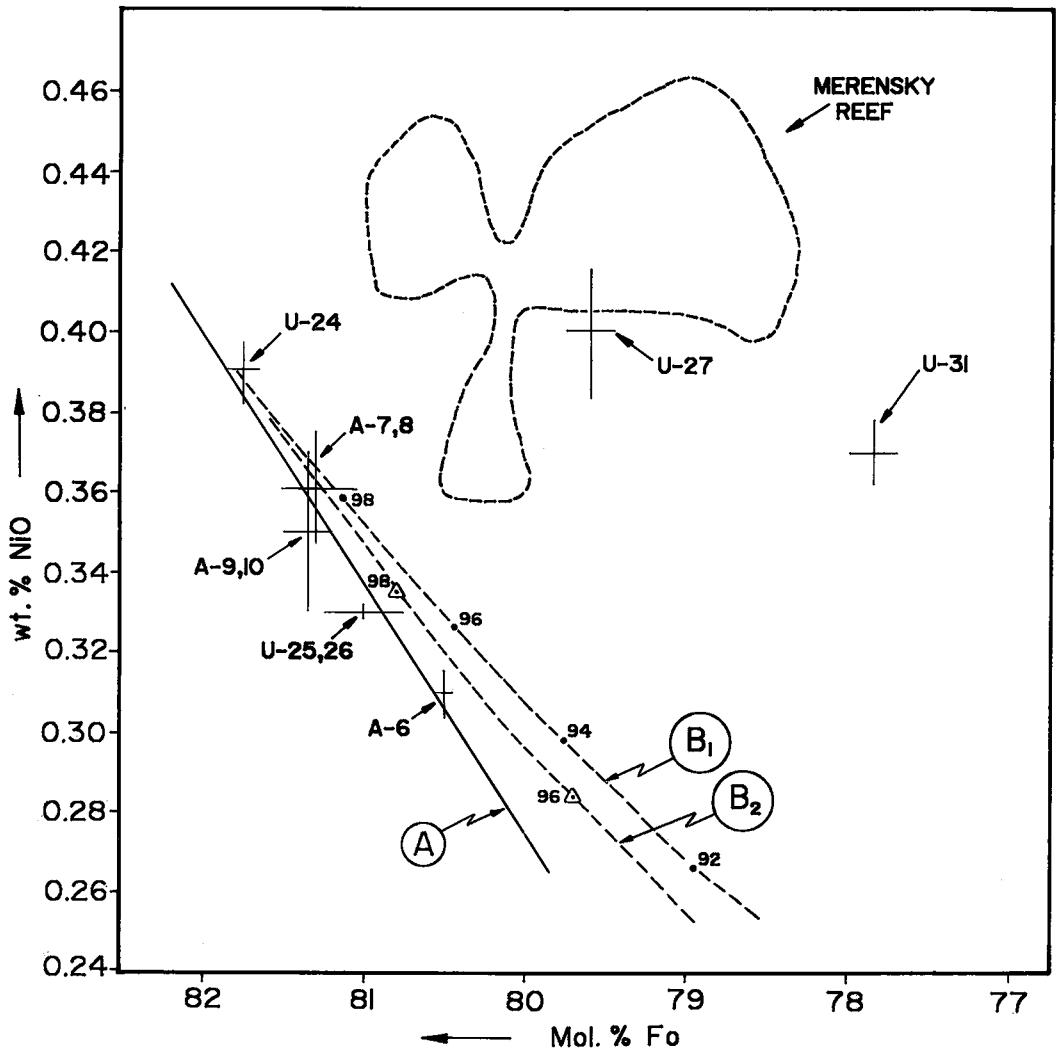

FIG. 10. Plot of wt.% NiO against mol.% Fo in olivine. Averages of each sample, excluding those from the Merensky Reef (enclosed area), are plotted as error bars that represent ± one standard deviation from the mean (Table 2). Samples from the Upper Pseudoreef – Footwall package (U-24,25,26 and A-6,7,8,9,10) fit a regression line "A" (NiO = [Fo • 0.0633] – 4.7932, correlation coefficient = 0.97, number of samples = 37) that approximates theoretical fractionation-curves (B_1, B_2) calculated assuming the initial liquid (containing 15 wt.% MgO and 10 wt.% MgO in B_1 and B_2, respectively) was in equilibrium with sample U-24 ($Fo_{81.76}$; 0.39 wt.% NiO). Both B_1 and B_2 are plotted at crystallization intervals of 2%.

indication of the abnormal concentration of incompatible and volatile elements), and, of course, by the concentration of BMS and PGE mineralization.

Composition of olivine

Representative compositions derived by electron-microprobe analysis of olivine from the cumulates described above are presented in Table 2. These data are plotted on diagrams of height against mol. % Fo (Figs. 3, 4) and wt. % NiO against mol. % Fo (Fig. 9). These compositions refer to the core zone of grains, but actually no within-grain zonation was detected. These data plot in several fields and do not, as might be expected from samples from such a limited height in a cumulate pile, define a single population (Fig. 9). If these data are categorized into cyclic units, four principal groups may be identified namely the UG-2 cyclic unit (sample U-31), the Lower Pseudoreef cyclic unit (sample U-27), the Upper Pseudoreef – Footwall cyclic units (samples U-24,25,26 and A-6,7,8,9,10) and the Merensky cyclic unit (samples U-15,15A,16 and A-2,3,4,5) (see also Fig. 10). Samples from the Lower Pseudoreef could be grouped with samples from the Merensky Reef, but it must be remembered that these two cumulates are separated by at least two other cyclic units. Compositional differences in olivine from the Upper Pseudoreef – Footwall package (comprising up to four cyclic units) are explained by a fractional-crystallization model (see below).

Olivine from the Merensky Reef is slightly richer in Ni and exhibits a much wider range of variation in both Ni and Fo contents in comparison with olivine from sulfide-poor cumulates (Figs. 9, 10). The variability is outside the analytical precision (± 0.01 wt. % NiO) and is attributed to grain-to-grain differences. Barnes & Naldrett (1985) reported similar features in olivine from the sulfide-rich J-M Reef in the Stillwater Complex.

Whole-rock chemistry

Major elements. Whole-rock compositions of some of the olivine-bearing cumulates analyzed in this study are presented in Table 1. A triangular plot of normative olivine–plagioclase–pyroxene (Fig. 7A) illustrates some of the mineralogical variations evident from petrographic studies, *e.g.*, the presence of > 10 modal % plagioclase in all of the "ultramafic" cumulates and the greater proportion of olivine in the poikilitic harzburgites as compared with the granular harzburgites. Whole-rock data for MgO, FeO, CaO, Na_2O and K_2O allow these ultramafic cumulates to be divided into at least two groups: the Upper Pseudoreef – Footwall package and the Merensky cyclic unit (Fig. 7B). Scatter within these samples groups is attributed to differences in Mg/Fe^{2+} ratio between coexisting olivine and orthopyroxene. Samples from the UG-2 and Lower Pseudoreef cyclic units (two samples only) plot between these two groups. Felsic cumulates from the Upper Pseudoreef – Footwall package and Merensky cyclic unit also plot as two discrete groups on this diagram, both defining linear trends related to modal variation (Fig. 7C). However, samples from the Merensky cyclic unit are relatively more fractionated (as defined by a decrease in the Mg/Fe^{2+} ratio); it

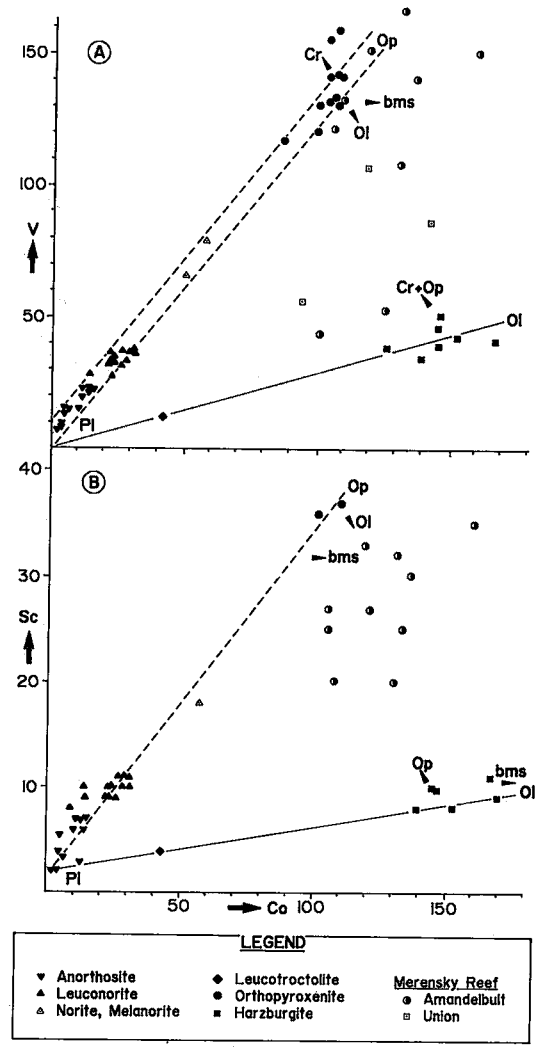

FIG. 11. Plots of ppm V against ppm Co (A) and ppm Sc against ppm Co (B). Each symbol represents one whole-rock composition. Linear trends reflect modal variations related to plagioclase (Pl) – orthopyroxene (Op) and plagioclase – olivine (Ol) control lines. Scatter from these trends is caused by accessory olivine, orthopyroxene, chromite (Cr) and base-metal sulfide (bms).

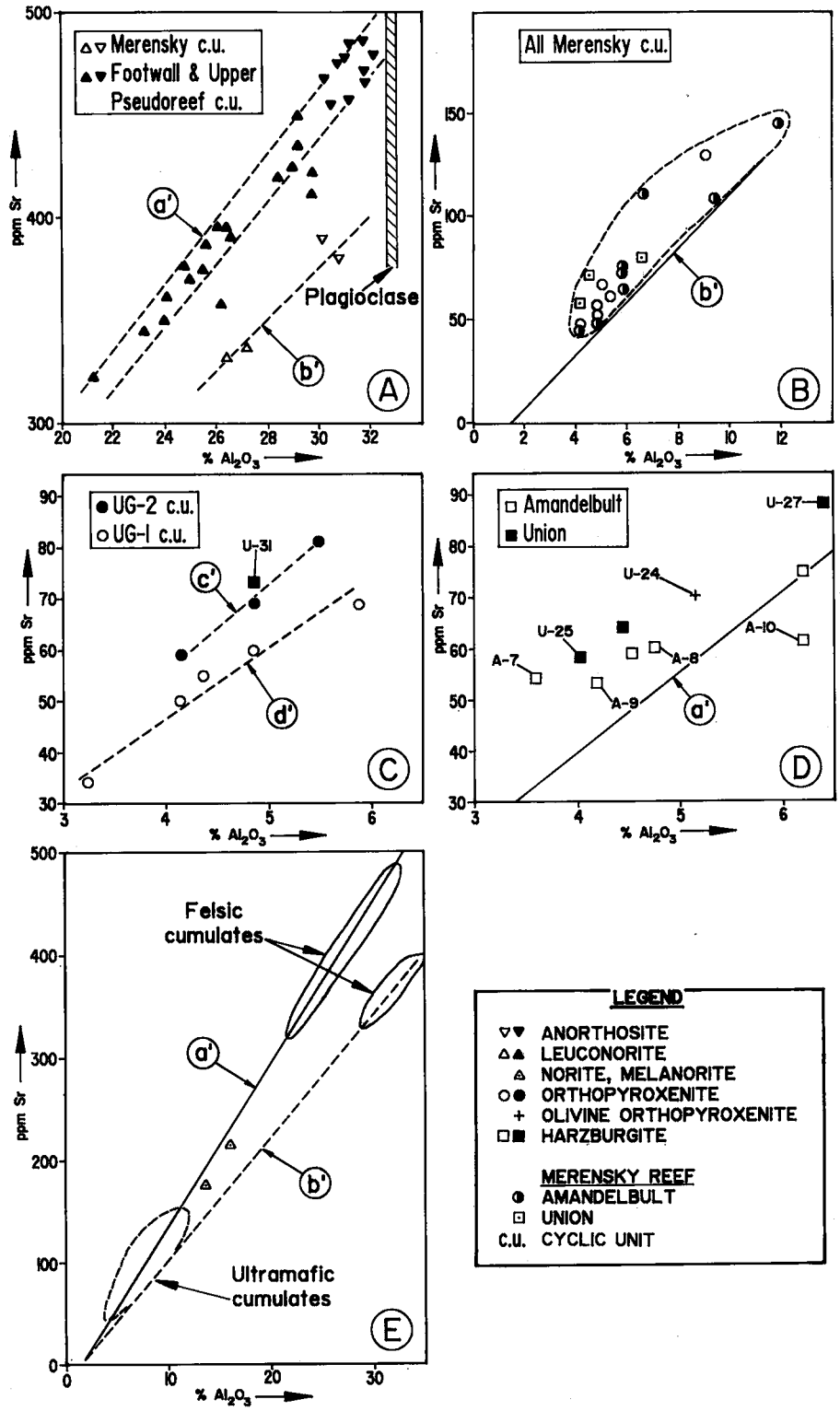
Merensky c.u.
Footwall & Upper Pseudoreef c.u.
a'
b'
Plagioclase
A
ppm Sr
% Al2O3
All Merensky c.u.
B
UG-2 c.u.
UG-1 c.u.
U-31
c'
d'
C
Amandelbult
Union
U-27
U-24
U-25
A-10
A-7
A-8
A-9
D
Felsic cumulates
Ultramafic cumulates
E
LEGEND
ANORTHOSITE
LEUCONORITE
NORITE, MELANORITE
ORTHOPYROXENITE
OLIVINE ORTHOPYROXENITE
HARZBURGITE
MERENSKY REEF
AMANDELBULT
UNION
C.U. CYCLIC UNIT

is concluded that both ultramafic and felsic cumulates in these two groups are compositionally discrete. It is also significant that both felsic and ultramafic cumulates from the different cyclic units in the Upper Pseudoreef – Footwall package do not exhibit any discernable trends of fractionation.

Trace elements: The distribution of Co, Sc and V in ultramafic and felsic cumulates is illustrated in Figure 11. These trace elements (together with Cr) partition preferentially into orthopyroxene, with lesser amounts in olivine, and are essentially rejected by plagioclase in olivine–orthopyroxene–plagioclase cumulates. Their distribution, at least in these samples, reflects modal variations, and they are not sensitive indicators of subtle compositional differences between adjacent cyclic units. The distribution of Cr is controlled principally by chromite, minor quantities of which influence whole-rock compositions.

Strontium partitions almost exclusively into plagioclase in olivine–orthopyroxene–plagioclase cumulates, the Sr content of which appears to be very sensitive to the composition of the primary magma (Eales *et al.* 1983, Kruger & Marsh 1985, Eales 1987). Kruger & Marsh (1985) obtained values of 480, 430 and 400 ppm Sr for plagioclase in the Footwall, Merensky and Bastard cyclic units, respectively, at the Rustenburg Section mine of RPM. Similar values are calculated for the Upper Pseudoreef – Footwall package and Merensky cyclic unit in this study (Fig. 12A). These data are subject to errors due to within-grain zonation and chemical differences between cumulus and intercumulus grains (features recognized by Kruger & Marsh 1985). Intercumulus plagioclase in ultramafic cumulates from different cyclic units, *e.g.*, the UG–1 and UG–2, also appears to be characterized by discrete Sr contents (Fig. 12C). Moreover, it is evident that intercumulus plagioclase in ultramafic cumulates is relatively richer in Sr than cumulus plagioclase in felsic cumulates (compare samples in Figs. 12B and 12D with those in Fig. 12A).

In the rocks in this study Cu behaves as an almost perfect chalcophile element; its distribution is directly related to the presence of BMS, and it is incompatible with respect to the other cumulus phases (Fig. 13). The low levels of Cu found in felsic cumulates, which may be slightly richer in Cu than sulfide-poor ultramafic cumulates, are attributed to microscopic specks of sulfide. Naldrett *et al.* (1983) reported that orthopyroxene in the Merensky cyclic unit contains about 700 ppm Ni, such that values in excess of this in whole-rock samples are attributed to BMS. If this "excess" Ni is plotted against Cu, the Ni/Cu ratio of the sulfide is obtained. In the rocks in this study, sulfide control becomes evident in orthopyroxenites that contain over 800 ppm Ni and in harzburgites that contain over 1800 ppm Ni (Fig. 13), and the Ni/Cu sulfide ratio may be estimated at between 1 and 2 (Naldrett *et al.* 1983 obtained values of 2.3 and 1.2 for the Merensky Reef and the remainder of the Merensky cyclic unit, respectively).

In contrast, the distribution of Ni and Co is influenced by both ferromagnesian silicates and BMS (Fig. 14). The sulfide control of Ni in the Merensky cyclic unit described by Lee (1983) is not generally applicable; the Merensky cyclic unit is clearly exceptionally sulfide-rich (Fig. 3). The Ni/Co ratio of sulfide-poor plagioclase–orthopyroxene cumulates in this study is estimated to be 6 (trend a′, Fig. 14), but in sulfide-poor harzburgites this ratio increases to over 40 (lower part of trend c′), a function of the much greater D^{Ni}(oliv/liq) in comparison to D^{Ni}(opx/liq). Orthopyroxene–sulfide (trend b′) and olivine–sulfide (trend c′) control lines are subparallel with the sulfide-poor harzburgite control line, and it is concluded that $K_D^{Ni/Co}$(oliv/liq) and $K_D^{Ni/Co}$(sulf/liq) are comparable. Data in this study are not sufficiently detailed to identify whether different cyclic units exhibit discrete Ni/Cu and Ni/Co sulfide ratios or Ni/Co whole-rock ratios.

Naldrett *et al.* (1983) suggested that incompatible elements such as Nb, Zr, Y and Rb may be used as indicators of the amount of trapped intercumulus material. In this study ratios of incompatible elements are reasonably constant and do not differ from one cyclic unit to the next (Fig. 4). However, ultramafic cumulates, and in particular pegmatoidal layers such as the Merensky Reef, may be richer in the incompatible elements than felsic cumulates (Figs. 3,4). Naldrett *et al.* (1983) attributed this feature to porosity control, but it may also be explained by trapping of upward-migrating intercumulus liquid (see Irvine 1980).

FIG. 12. Plots of ppm Sr against wt.% Al_2O_3. Each symbol represents one whole-rock composition. (A) Felsic cumulates from the Upper Pseudoreef – Footwall package and Merensky cyclic unit define separate regression lines, a′ (Al_2O_3 = [Sr•0.063] + 1.543; correlation coefficient = 0.986; number of samples = 28) and b′ (four data points only), respectively. From knowledge of the Al_2O_3 content of plagioclase (hatched area), the Sr content of plagioclase (cumulus + intercumulus) is estimated as 480 ppm (a′) and 400 ppm (b′). (B) Ultramafic cumulates from the Merensky cyclic unit plot above the regression line b′ (calculated assuming that pure plagioclase contains 400 ppm Sr and the intercept = 1.543 wt.% Al_2O_3). (C) Ultramafic cumulates from the UG–2 and UG–1 cyclic units define separate linear trends, c′ and d′. (D) Ultramafic cumulates from the Pseudoreef multiunit and Footwall cyclic unit plot above the regression line a′. (E) Ultramafic and felsic cumulates from the Upper Pseudoreef – Footwall package (a′) and Merensky cyclic unit (b′).

Summary. (1) A compositional break occurs at the level of the Merensky Reef. (2) Two compositionally discrete groups of cumulates, ultramafic and felsic, occur in the Upper Pseudoreef – Footwall package. However, although this package comprises up to four cyclic units, the composition of both groups of cumulates is consistent throughout; it is concluded that each group is related to a separate magma, or separate fractional-crystallization derivatives of one primary magma.

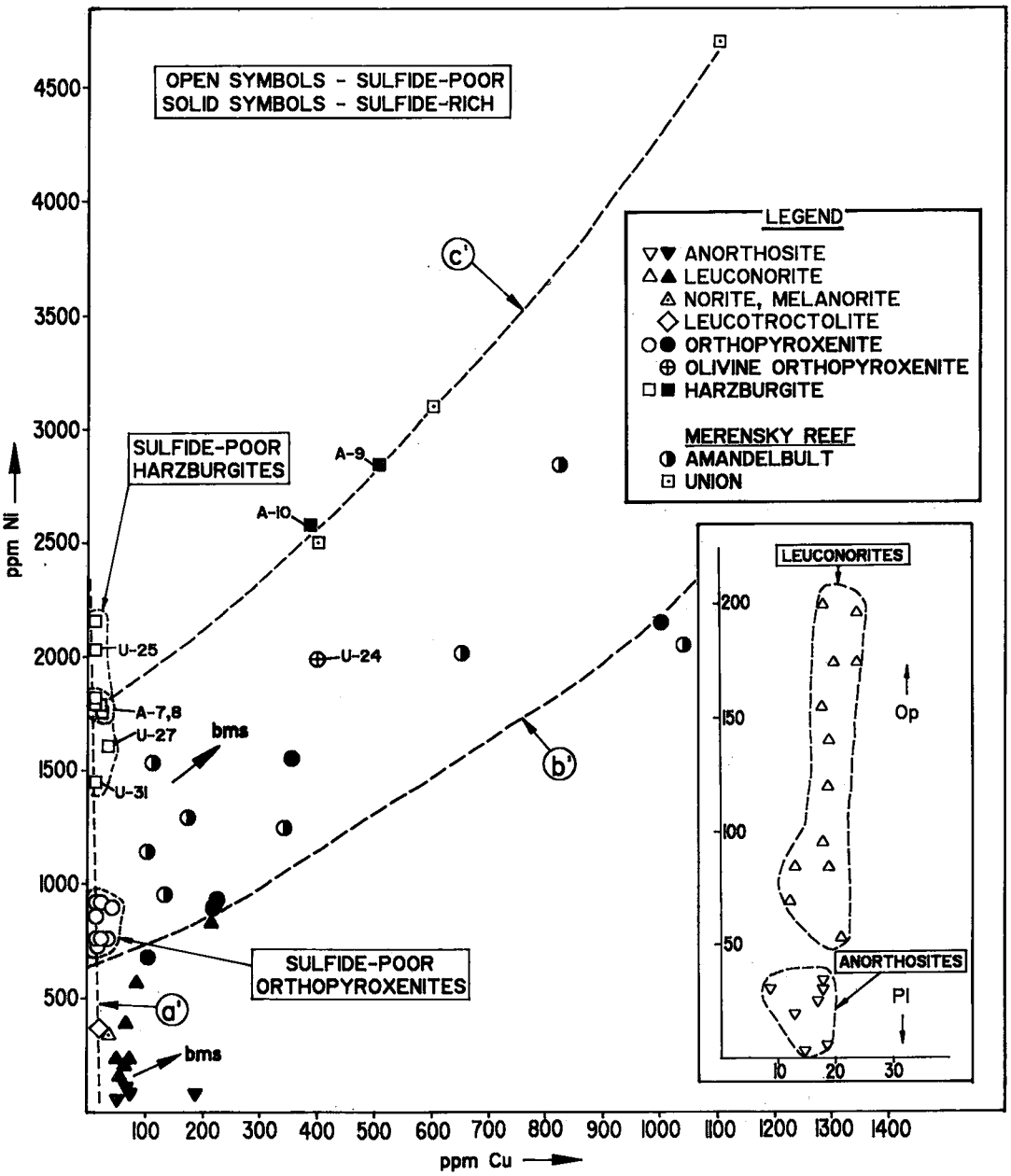

FIG. 13. Plot of ppm Ni against ppm Cu. Each symbol represents one whole-rock composition. Sulfide-poor samples (open symbols) define a linear trend a′ (for felsic end, see inset; op orthopyroxene, pl plagioclase). Sulfide-rich samples (solid symbols and Merensky Reef samples) define two trends, orthopyroxene–sulfide (b′) and olivine–sulfide (c′) control lines. Samples between b′and c′ (shaded area) contain orthopyroxene, olivine and sulfide.

Base-Metal Sulfide and Platinum-Group Element Mineralization

Distribution

UG-2 cyclic unit. The UG-2 "Reef" is now considered to be of equal importance to the Merensky Reef as a mineable reserve of PGE. McLaren & De Villiers (1982) described the UG-2 chromitite layer as "containing only a small amount of sulfide highly enriched in PGE", and Naldrett & Cabri (1976) and Naldrett (1981) reported that the UG-2 Reef has exceptionally high chondrite-normalized PGE contents. The UG-2 layer is characterized by high Ni/Fe and Cu/Fe sulfide ratios (pentlandite and chalcopyrite are dominant over pyrrhotite), although the Cu/(Cu + Ni) sulfide ratio is comparable to that in the Merensky Reef (McLaren & De Villiers 1982). BMS are only rarely observed in the remainder of the UG-2 cyclic unit, and PGE only occur at the base of the unit, closely associated with the main chromitite layer.

Pseudoreef multiunit. Significant, although subeconomic, concentrations of BMS and PGE occur in and for 2.0 cm above and below the chromitite layer that separates the Lower and Upper Pseudoreefs at the Union Section mine, and in the Lower Pseudoreef and Upper Pseudoreef A at the Amandelbult Section mine. However, the harzburgite layers that comprise the Upper Pseudoreefs at both mines are very poor in sulfide (whole-rock samples contain <20 ppm Cu; Table 1) and, as far as we are aware, contain no significant concentrations of PGE. The Lower Pseudoreef at the Amandelbult Section mine, a pegmatoidal, feldspathic orthopyroxenite, may be considered as a subeconomic equivalent of the Merensky Reef.

Footwall cyclic unit. The olivine-rich cumulates and the chromitite layer at the base of the Footwall cyclic unit at the Union Section mine contain anomalous concentrations of BMS and PGE. No data are available on the equivalent interval at the Amandelbult Section mine.

Merensky cyclic unit. BMS and PGE mineralization is essentially restricted to ultramafic cumulates at the base of the Merensky cyclic unit, comprising the Merensky pegmatoid, the lower and upper chromitite layers and the lower part of the Merensky (hangingwall) pyroxenite. Maximum concentrations of PGE in the Merensky package at both the Amandelbult Section and Union Section mines occur either in, or in close association with, the two chromitite layers (particularly in the upper chromitite layer; Viljoen *et al.* 1986a, b). PGE occur to a lesser extent in the pegmatoidal layer between the two chromitite layers and for a few centimetres upward into the hangingwall pyroxenite. The footwall contact is sharp, and the Merensky (footwall) anorthosite is essentially devoid of PGE and BMS. In contrast, BMS are concentrated in the pegmatoidal layer and in the hangingwall pyroxenite (for between 10 and 20 cm above the upper chromitite layer) and not in the chromitite layers, such that maximum Ni and Cu sulfide values occur in the hangingwall pyroxenite, above the PGE orebody.

Summary. The distribution of BMS and PGE mineralization in the study section may be summarized as follows: (1) BMS and PGE mineralization is not restricted to the UG-2 and Merensky Reefs; some of the ultramafic cumulates between these two

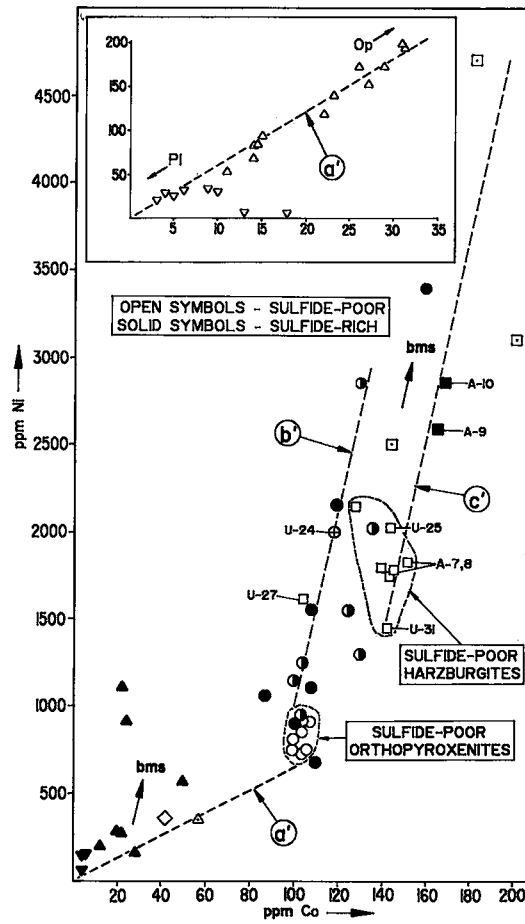

FIG. 14. Plot of ppm Ni against ppm Co. Each symbol represents one whole-rock composition analysis. Legend as for Figure 13. Sulfide-poor samples (open symbols) of plagioclase (pl) – orthopyroxene (op) cumulates define a linear trend a′ (for felsic end, see inset). Sulfide-rich samples (solid symbols and Merensky Reef samples) define two linear trends, orthopyroxene–sulfide (b′) and olivine–sulfide (c′) control lines, respectively. Samples between b′ and c′ (shaded area) contain orthopyroxene, olivine and sulfide.

layers also contain significant mineralization. (2) BMS mineralization is preferentially concentrated in olivine–orthopyroxene cumulates with a pegmatoidal texture; lesser amounts occur in certain chromitite layers. (3) PGE mineralization is concentrated in certain (but not all) chromitite layers and stringers, with lesser amounts in olivine–orthopyroxene cumulates with a pegmatoidal texture. (4) BMS and PGE mineralization always occurs in ultramafic cumulates at, or near, the base of cyclic units, whereas mafic and felsic cumulates are essentially devoid of BMS and PGE mineralization.

Base-metal sulfide mineralogy of the Merensky Reef

The principal BMS in the Merensky Reef in the western Bushveld Complex, in order of decreasing abundance, are pyrrhotite, pentlandite, chalcopyrite and pyrite (Liebenberg 1970, Van Zyl 1970, Von Gruenewaldt 1979). The low sulfide content [0.5 – 2.0 wt. % according to Cousins (1969) and 2.75 wt. % according to Vermaak & Hendriks (1976)] and the high Ni/Fe and Cu/Fe sulfide ratios are unusual for magmatic ores (Cousins 1969). From the data of Vermaak & Hendriks (1976), who studied the reef at the Rustenburg Section mine of RPM, the following normative sulfide contents are calculated: 39.6% pyrrhotite, 22.2 % pentlandite, 16.4% chalcopyrite and 21.8% pyrite. The normative sulfide content of the reef at the Western Platinum mine (see Fig. 1), calculated from the data of Brynard *et al.* (1976), is as follows: 50.2% pyrrhotite, 34.3% pentlandite, 10.6% chalcopyrite and 4% pyrite. Reflected-light studies of BMS in the study sections confirm that it is typical of the reef in the western Bushveld Complex.

The results of an electron-microprobe study of BMS in the Merensky Reef at the Amandelbult Section mine, together with some data from the literature, are presented in Table 3. The pyrrhotite is typically an intergrowth of the hexagonal and monoclinic varieties, although troilite occurs rarely. The pentlandite is an extremely Co-poor variety and is further distinguished by a low Ni/Fe ratio. The association of hexagonal and monoclinic pyrrhotite and Co-poor pentlandite is characteristic of certain magmatic ores, according to Harris & Nickel (1972).

Discussion: the Ni Content of Olivine

Compositional differences between olivine from different cyclic units may be attributed to fractional crystallization, to the influence of sulfide, to the formation of a pegmatoidal texture, or to differences in initial composition of the liquid.

Fractional crystallization

Theoretical olivine-fractionation curves can be generated for a range of initial composition of liquid using the reaction of Roeder (1974), *i.e.*, $K_D = [(X_{MgO})/(X_{FeO})]^{liq.} \cdot [(X_{FeO})/(X_{MgO})]^{oliv}$, where X_{MgO} and X_{FeO} are mole fractions and K_D equals 0.3, and calculating the distribution of Ni between olivine and liquid (D^{Ni}) from the formulae of Hart & Davis (1978), *i.e.*, $D^{Ni} = [124.13/(MgO^{liq})] - 0.897$, where

TABLE 3. CHEMICAL COMPOSITION OF BASE-METAL SULFIDES IN THE MERENSKY REEF*

	1		2		3		4		5	6	7
wt.%	x̄	s	x̄	s	x̄	s	x̄	s			
S	36.50	.186	38.96	.035	37.90	.690	33.59	.314	31.86	35.21	33.10
Fe	64.18	.393	62.45	.339	59.90	.540	34.48	.847	32.95	31.08	30.50
Co	n.d.	-	n.d.	-	0.10	-	0.28	.180	0.90	-	-
Ni	n.d.	-	n.d.	-	0.20	-	30.78	1.162	33.55	-	-
Cu	-	-	-	-	n.d.	-	-	-	-	33.34	33.70
TOTAL	100.68		101.41		98.10		99.13		99.25	99.75	97.30
at.%											
S	49.78		52.08		52.37		47.75		45.81	50.35	49.00
Fe	50.22		47.92		47.45		28.14		27.16	25.31	25.90
Co	-		-		0.06		0.22		0.69	-	-
Ni	-		-		0.12		23.89		26.34	-	-
Cu	-		-		-		-		-	24.14	25.10
n	3		2		3		9		2	7	1
M:S	1.009		.920		.909		8.75		9.40	-	-

n : number of samples; x : mean; s : standard deviation; n.d. : not determined.
M:S ratio = (Fe+Co+Ni)/S, S=8 for pentlandite.
1 - Troilite; 2,3 - Hexagonal pyrrhotite; 4,5 - Pentlandite; 6,7 - Chalcopyrite.
Compositions 1,2,4,6 - this study; Compositions 3,5,7 from Vermaak & Hendriks (1976).
* Determined by electron microprobe analysis.

MgO^{liq} is in wt.%. Several major assumptions are made; firstly, the initial liquid is considered in equilibrium with the most primitive olivine in the data set, and secondly it is necessary to assume the MgO content of the liquid (see caption to Fig. 10). It is concluded that samples from the Upper Pseudoreef - Footwall package may be fitted to a theoretical fractionation path, but samples from the UG-2, Lower Pseudoreef and Merensky cyclic units do not fit a common model of fractionation (Fig. 10).

TABLE 4. K_D FOR THE MERENSKY REEF

	n	NiO/FeO	$(K_D)^1$	$(K_D)^2$
UNION SECTION				
U-15	5	0.0241	6	9
U-15A	3	0.0222	7	10
U-16	6	0.0208	7	11
AMANDELBULT SECTION				
A-3	12	0.0213	7	10
A-5	10	0.0225	7	10

n : number of analyses of olivine.
$(K_D)^1$: NiS/FeS = 0.15; $(K_D)^2$: NiS/FeS = 0.22

The influence of sulfide and a pegmatoidal texture

Distribution of Ni and Fe between olivine and molten sulfide. The distribution of Ni and Fe between olivine and molten sulfide may be expressed as the partition coefficient $K_D^{Ni/Fe}$(sulf/oliv), where $K_D = [(X_{NiS})/(X_{FeS})]^{sulf.} \cdot [(X_{FeO})/(X_{NiO})]^{oliv}$ (Thompson *et al.* 1984). Thompson *et al.* quoted an average K_D of 9.8 for natural assemblages, which is consistent with the findings of Duke & Naldrett (1978), Naldrett (1979), Boctor (1982) and Barnes & Naldrett (1985) but conflicts with the high values (> 30) obtained experimentally by Fleet *et al.* (1977, 1981) and Fleet & Macrae (1983) (see discussions by Fleet 1979, Naldrett 1979, 1981, Thompson *et al.* 1984, Barnes & Naldrett 1985). The accurate determination of the composition of the sulfide fraction of disseminated ores presents a problem (Thompson *et al.* 1984), and we have estimated the NiS/FeS ratio of the sulfide fraction in the Merensky Reef by combining the normative sulfide data of Vermaak & Hendricks (1976) (NiS/FeS = 0.15) and of Brynard *et al.* (1976) (NiS/FeS = 0.22) with the chemical compositions of discrete sulfide phases presented in Table 3. The NiO/FeO ratio of olivine is calculated from data in Table 2, and it is concluded that K_D for the Merensky Reef in the western Bushveld Complex varies between 6 and 11 (Table 4). These results are consistent with values for K_D of 11.4 and 9.7 for the J-M Reef in the Stillwater Complex obtained by Thompson *et al.* (1984) and Barnes & Naldrett (1985), respectively. It is concluded that the Merensky Reef is characterized by the association of Ni-rich olivine with Ni-rich sulfide.

Re-equilibration and the high "R value" model. In massive-sulfide ores, it may be predicted that subsolidus re-equilibration will modify liquidus compositions, but in disseminated ores this process is less likely to have influenced the composition of olivine. Moreover, if much of the sulfide is located within intercumulus plagioclase (Fig. 8d), the composition of the sulfide fraction may remain unaffected. Clark & Naldrett (1972) obtained a value of 33.2 ± 3.4 for the distribution of Ni and Fe between olivine and monosulfide solid solution. The low value of K_D obtained in this study, together with the above observations, argue that K_D is a measure of either primary liquidus compositions or the result of equilibration at magmatic temperatures. Barnes & Naldrett (1985) also rejected subsolidus re-equilibration as a mechanism to explain their data on the J-M Reef and suggested two alternative hypotheses: equilibration during crystallization of trapped (intercumulus) liquid (a hypothesis that they eventually discarded) and equilibration during magma mixing and gravity settling of the molten sulfide droplets.

The pegmatoidal texture of the Merensky Reef may be evidence that the K_D was influenced by reaction between olivine and sulfide during crystallization of a substantial proportion of intercumulus liquid (note that the reef is characterized by unusually high contents of incompatible elements). However, the Ni content of the Merensky Reef olivine is only marginally higher than that of olivine from non-pegmatoidal cumulates; consequently, this process may be regarded as having only a minor influence.

The second hypothesis of Barnes & Naldrett (1985) and the models of Campbell *et al.* (1983) and Campbell & Barnes (1984) draw on the influence of a high *"R"* value", the bulk silicate/sulfide liquid ratio as defined by Campbell & Naldrett (1979). If the *R* value is much larger than D^{Ni} (sulf/liq), *e.g.*, greater than 2500, separation of a small proportion of sulfide will produce no discernable depletion of Ni in the melt; accordingly, the Ni content of coexisting olivine will remain unaffected. Settling of immiscible sulfide droplets through a large volume of liquid is invoked as a mechanism to obtain the large value of *R*. Some problems with this model are discussed later, but first we present an alternative hypothesis to account for the association of Ni-rich olivine with Ni-rich sulfide in the Merensky Reef.

Stage at which saturation in S is reached. Two major criticisms against models that explain the origin of Ni sulfide ores by magmatic immiscibility are that coexisting olivine is commonly enriched in Ni, not depleted as may be expected, and that magmatic sulfides exhibit a wide range in Ni/Fe (and Ni/Cu) sulfide ratios. These features may be

explained by considering the stage at which saturation in S is reached in the magma (Rajamani & Naldrett 1978, Duke & Naldrett 1978, Duke 1979). If an immiscible sulfide phase segregates after crystallization of olivine, the monosulfide liquid solution (*mls*) will be depleted in Ni (the Ni content of the olivine will be normal); but if the reverse situation occurs, the *mls* will be Ni-rich, and the olivine will be depleted in Ni. However, if saturation in S is concomitant with crystallization of olivine, the distribution of Ni and Fe will be controlled entirely by K_D (ignoring subsolidus effects and the influence of a high value of R), and it may be predicted that the Ni/Fe ratio of coexisting olivine and sulfide will exhibit a positive correlation (as shown by the data of Barnes & Naldrett 1985). It may then be predicted that if the sulfide is Ni-rich (as in the Merensky Reef), the coexisting olivine will also be Ni-rich.

The causes of saturation in S are not fully known, but magma mixing, decrease in temperature, fractional crystallization, changes in $f(O_2)$ and $f(S_2)$ and magma composition (particularly in the Fe^{2+} content) are some of the proposed mechanisms (Haughton *et al.* 1974, Shima & Naldrett 1975, Naldrett 1981). The relative proportions of Fe, S and O within the *mls* are probably tightly controlled in a large magma-chamber, whereas this is not true of minor components such as Ni, Cu and *PGE* (Naldrett 1981), such that the relative height in a layered complex is an important factor in determining the presence of Ni-rich sulfides.

Differences in initial composition of the liquids

From the above discussion, it is concluded that differences in the Ni content of olivine from the UG–2 cyclic unit, Lower Pseudoreef cyclic unit, Upper Pseudoreef – Footwall package and Merensky cyclic unit are best explained by minor differences in initial composition of the liquids. The various olivine-bearing cumulates in the Upper Pseudoreef – Footwall package are related by a fractional-crystallization model. The magmas responsible for the UG–2, Lower Pseudoreef and Merensky cyclic units, it is believed, were saturated in S at an early stage, probably whilst olivine was still a liquidus phase. However, the batch of magma related to the ultramafic cumulates in the Upper Pseudoreef – Footwall package did not reach saturation in S prior to the mixing event (see below).

Formation of Cyclic Units in the Study Section

New influxes of magma

We argue that the presence of ultramafic cumulates in the cyclic units in the upper Critical Zone above the UG–1 chromitite layer is related to replenishment of the chamber by new influxes of magma. New influxes of magma, in each case distinguished by subtle compositional differences, are postulated to have occurred at the base of the UG–2, Lower Pseudoreef, Upper Pseudoreef and Merensky cyclic units. However, the Upper Pseudoreef – Footwall package is attributed to periodic tapping of one batch of magma. A consensus of opinion suggests that chromitite layers form as a result of magma mixing (Irvine & Sharpe 1983, Eales & Reynolds 1983, Hatton & Von Gruenewaldt 1983) such that new magma influxes may be responsible for all of the cyclic units in the study section with basal chromitite layers. The reappearance of magnesian olivine and the recurrence of major chromitite layers imply that these new influxes of magma were relatively primitive in comparison with the column of supernatant liquid, and may be comparable to the magma in the chamber during crystallization of the lower Critical Zone. However, our data do not allow us to be more specific as to the exact composition of the putative magmas.

Crystallization of large amounts of plagioclase from a tholeiitic magma results in increased density of the residual magma (Huppert & Sparks 1980, Campbell *et al.* 1983, Sparks & Huppert 1984). Eventually, a "density-crossover point" occurs, at which stage the residual magma is denser than a new (more primitive) magma. The models of Campbell *et al.* (1983), Campbell & Barnes (1984) and Barnes & Naldrett (1985), that argue in favor of a high value of R, require that this crossover point was reached at the level of the Merensky Reef (and J–M Reef). We believe that their argument is equivocal and prefer to assume that the new influxes of magma would still be denser than the residual magma in the chamber at this level. We postulate that each new influx intrudes the chamber as a flow along the crystal–liquid interface, as described by the models of Huppert & Sparks (1980) and Sparks & Huppert (1984), and does not intrude as a jet or buoyant plume as suggested by Campbell *et al.* (1983). Temperature and density differences between the new, relatively hot and dense magma and the column of supernatant liquid result in the formation of a stratified layer at the base of the chamber. The new influx of magma sharply truncates the previous cyclic unit and may partially resorb the uppermost layer of crystals. As the new magma begins to cool, fractional crystallization [probably dominantly bottom crystallization as described by McBirney & Noyes (1979), but possibly with some cumulus mineral formation with settling over a few metres] results in the formation of an ultramafic cumulate at the base of the developing cyclic unit.

Cyclic units

We reported earlier that three types of cyclic units

occur in the study sections. Cyclic units that consist entirely of ultramafic cumulates (the UG–1, UG–2 and Lower Pseudoreef at both mines, the Upper Pseudoreef at the Union Section mine and the Upper Pseudoreef C at the Amandelbult Section mine) are attributed to fractional crystallization of the stratified layer of new magma as a separate entity; the developing cyclic unit is then terminated at an early stage by a further influx of magma.

Hybrid cyclic units, that consist of ultramafic cumulates at the base that are sharply overlain by felsic cumulates (the Footwall at both mines and the Upper Pseudoreef A and B at the Amandelbult Section mine), are explained by the following hypothesis. As cooling and fractional crystallization proceed, density differences between the new magma and the column of supernatant liquid will be eradicated, such that the liquid stratification will break down, and the new and residual magmas will mix. The ultramafic cumulates crystallize from the new influx of magma, and the felsic cumulates crystallize from the blended magma, after the mixing event. Eradication of stratification in the liquid explains why complete cyclic units are not observed in the study sections (note that even the most complete cyclic units in the upper Critical Zone are capped by anorthosites and iron-rich gabbros, and other more fractionated cumulates are not observed until the Upper Zone). The stage at which the two magmas mix will determine the sequence of cumulates in the hybrid cyclic unit. This hypothesis accounts for the presence of two discrete types of cumulates (ultramafic and felsic), the absence of mafic cumulates, compositional differences between the two types of cumulates in one cyclic unit (that cannot be attributed to modal effects or fractional crystallization), and disequilibrium contacts within cyclic units. This hypothesis relies on the new influx of magma being volumetrically small, so that after the mixing event the liquidus relationships of the blended magma are comparable to those in the column of supernatant liquid (it will be remembered that felsic cumulates in different cyclic units in the Upper Pseudoreef – Footwall package are compositionally identical).

Formation of the Merensky and Bastard cyclic units, the third type of cyclic unit in the study sections, is attributed to fractional crystallization of the new influx of magma as a discrete entity, the mixing only occurring after crystallization of the leuconorite layer (see Kruger & Marsh 1982, 1985).

Strontium-isotope systematics and the two-magma model

From strontium-isotope studies, Kruger & Marsh (1982) and Sharpe (1985) argued that a major new influx of magma (with initial $^{87}Sr/^{86}Sr$ ratio *ca.* 0.7085) intruded the chamber (residual magma with initial $^{87}Sr/^{86}Sr$ ratio *ca.* 0.7065) at some stage between the Merensky Reef and the Bastard Reef. The two-magma model of Irvine *et al.* (1983), Irvine & Sharpe (1983), Sharpe (1985) and Harmer & Sharpe (1985) is becoming increasingly accepted; therefore, it may be speculated that the ultramafic cumulates in the cyclic units between the UG–2 chromitite layer and Merensky Reef are derivatives of their "U-type" magma series, and the felsic cumulates, of their "A-type" magma series. However, only limited strontium-isotope data are available for this sequence [Kruger & Marsh (1982): 5 samples; Sharpe (1985): 2 samples]; these data are restricted to the felsic cumulates, and no data are available for the ultramafic cumulates [see, however, Hamilton (1977) for data on the layered sequence below the UG–1 chromitite layer]. Consequently, whether the hybrid cyclic units in the study sections are derived from two discrete magma-series or whether they are derivatives by fractional crystallization (possibly with minor contamination) of one primary magma is equivocal. We also stress that our data do not support the hypothesis of Todd *et al.* (1982) and Irvine *et al.* (1983) that anorthosite cumulates are derivatives of a separate liquid. In contrast, anorthosites in the study sections are related intimately to leuconorite cumulates and are clearly more fractionated than ultramafic cumulates in the same cyclic unit.

Broad similarities between the ultramafic cumulates immediately above and below the Merensky Reef (including the presence of PGE and BMS mineralization) suggest to us that the sequence between the UG–1 chromitite layer and the top of the Bastard cyclic unit should be assigned to one zone (the Critical Zone, not the Main Zone), even though the chamber at this level was evidently replenished by several new influxes of magma (which, if anything, we would equate with the U-type series, not the A-type series). To segregate the sequence at the level of the Merensky Reef, as the models of Kruger & Marsh (1985) and Sharpe (1985), amongst others, infer is to us unacceptable. Rather we would argue that the "major compositional break" occurs at the top of the Bastard cyclic unit, at the base of Main Zone as originally defined by Hall (1932). If the base of the Main Zone is positioned at the base of the Merensky Reef, the two major PGE orebodies are assigned to different zones and would presumably have to be explained by two separate hypotheses, as the UG–2 Reef is apparently not associated with cumulates with a high R_0 .

Base-metal sulfide and platinum-group-element mineralization

The high R-value – gravity-settling model of Campbell *et al.* (1983) does not explain the distribution of BMS and PGE mineralization in the sequence

studied here. The bulk of the BMS mineralization occurs as very small grains, and settling of such small droplets through a thick column of liquid (particularly if the liquid is stratified) is difficult to envisage. Secondly, a gravity-settling process would not be sufficiently efficient to produce the observed distribution-trends. Data presented in this study are consistent with a hypothesis in which some of the postulated new influxes of magma reached saturation in S rapidly after the magma entered the chamber, prior to mixing with the supernatant liquid. It is also possible that saturation in S occurred during ascent or in a deep-level magma chamber [see also Buchanan & Nolan (1979)]. Sulfide that segregated from a new influx of magma during crystallization of the ultramafic cumulates (the sulfide droplets may have percolated through a few tens of metres) may be described as cumulus mineralization [see also Lee (1983)].

The close association of BMS mineralization with ultramafic cumulates that exhibit a pegmatoidal texture and are rich in incompatible and volatile elements suggests that some of the BMS is related to fractionated, intercumulus liquids (postcumulus mineralization). The distribution of the PGE clearly reflects deposition from upward-migrating liquid, not gravitational settling (Cousins 1969, Vermaak & Hendriks 1976, Brynard *et al.* 1976, Lee 1983); consequently the PGE mineralization is postulated to be largely postcumulus, although minor amounts (particularly of the more chalcophile PGE, *e.g.*, Pd) may have been scavenged by cumulus sulfide. The close spatial occurrence of a number of PGE-rich layers is also difficult to explain by the high-*R*-value model, whereas it may be argued that if the PGE were concentrated into intercumulus liquids during crystallization of the ultramafic cumulates in the Lower and Critical Zones, their present position may be attributed to deposition in favorable sites. This hypothesis thus invokes partial decoupling of the BMS and PGE mineralization.

The concentration of PGE in chromitite layers, that in comparison with adjacent silicate layers are poor in BMS, is difficult to explain by any other hypothesis. The reasons why chromite (or chromitite layers, to be specific) acts as a collector for PGE are not understood, although the association of PGE and chromite is well known (Wagner 1929, Razin 1976, Hiemstra 1979). Other features that support this hypothesis are the mineralogical data presented by Crocket *et al.* (1976) and Kinloch (1982) (*e.g.*, platinum-group minerals are intergrown with silicates and occur as discrete phases and alloys, and are not always associated with composite sulfide grains) and the variation in PGE/sulfide ratios observed between adjacent cumulate layers. Variation of interelement PGE ratios between adjacent layers may also be explained by deposition of selective PGE in specific environments, whereas the exceptionally high distribution-coefficients suggested by Campbell *et al.* (1983) should result in constant interelement PGE ratios at a given height in the cumulate pile.

Acknowledgements

The authors thank the managements of the Johannesburg Consolidated Investment Company and Rustenburg Platinum Mines for access to their properties, assistance with field work, and financial support. The geological staff of RPM, particularly Bruce Walters, Kobus Theron and Piet Coetzer, are thanked for their contribution. JCI staff who gave us every assistance are Morris and Richard Viljoen, Chris Lee, John Barry and Euan Kinloch. Both authors express their thanks to Professor Hugh Eales and Drs. Ivan Reynolds and Goonie Marsh for assistance during our studies at Rhodes University. Professor Hugh Eales is also thanked for improving an early draft of the manuscript and the referees, paticularly Dr. T.N. Irvine, are thanked for their contributions. Responsibility for the interpretations and hypotheses presented here lies with R.N.S. Further details on the study sections at the Union Section and Amandelbult Section mines can be obtained from W.J.K. (unpublished M.Sc. thesis, Rhodes University) and R.N.S. (unpublished Ph.D. thesis, Rhodes University).

References

Barnes, S.J. & Naldrett, A.J. (1985): Geochemistry of the J-M (Howland) Reef of the Stillwater Complex, Minneapolis adit area. I. Sulfide chemistry and sulfide–olivine equilibrium. *Econ. Geol.* **80**, 627-645.

Bence, A.E. & Albee, A.L. (1968): Empirical correction factors for the electron microanalysis of silicates and oxides. *J. Geol.* **76**, 382-403.

Boctor, N.Z. (1982): The effect of fO_2, fS_2 and temperature on Ni partitioning between olivine and iron sulfide melts. *Carnegie Inst. Wash. Year Book* **81**, 366-369.

Brown, G.M. (1956): The layered ultrabasic rocks of Rhum, Inner Hebrides. *Phil. Trans. Roy. Soc. London* **B 240**, 1-53.

Brynard, H.J., de Villiers, J.P.R. & Viljoen, E.A. (1976): A mineralogical investigation of the Merensky Reef at the Western Platinum mine, near Marikana, South Africa. *Econ. Geol.* **71**, 1299-1307.

Buchanan, D.L. & Nolan, J. (1979): Solubility of sulfur and sulfide immiscibility in synthetic tholeiitic melts and their relevance to Bushveld-complex rocks. *Can. Mineral.* **17**, 483-494.

BUTCHER, A.R., YOUNG, I.M. & FAITHFULL, J.W. (1985): Finger structures in the Rhum Complex. *Geol. Mag.* **122**, 491-502.

CAMERON, E.N. (1982): The upper critical zone of the eastern Bushveld Complex – precursor to the Merensky Reef. *Econ. Geol.* **77**, 1307-1327.

CAMPBELL, I.H. & BARNES, S.J. (1984): A model for the geochemistry of the platinum-group elements in magmatic sulfide deposits. *Can. Mineral.* **22**, 151-160.

_____ & NALDRETT, A.J. (1979): The influence of silicate:sulfide ratios on the geochemistry of magmatic sulfides. *Econ. Geol.* **74**, 1503-1506.

_____, _____ & BARNES, S.J. (1983): A model for the origin of platinum-rich sulfide horizons in the Bushveld and Stillwater Complexes. *J. Petrology* **24**, 133-165.

CLARK, T. & NALDRETT, A.J. (1972): The distribution of Fe and Ni between synthetic olivine and sulfide at 900°C. *Econ. Geol.* **67**, 939-952.

COUSINS, C.A. (1969): The Merensky Reef of the Bushveld Igneous Complex. *In* Magmatic Ore Deposits (H.D.B. Wilson, ed.). *Econ. Geol., Mon.* **4**, 239-251.

CROCKET, J.H., TERUTA, Y. & GARTH, J. (1976): The relative importance of sulfides, spinels, and platinoid minerals as carriers of Pt, Pd, Ir and Au in the Merensky Reef at Western Platinum Limited, near Marikana, South Africa. *Econ. Geol.* **71**, 1308-1323.

DUKE, J.M. (1979): Computer simulation of the fractionation of olivine and sulfide from mafic and ultramafic magmas. *Can. Mineral.* **17**, 507-514.

_____ & NALDRETT, A.J. (1978): A numerical model of the fractionation of olivine and molten sulfide from komatiite magma. *Earth Planet. Sci. Lett.* **39**, 255-266.

EALES, H.V. (1987): The features and genetic significance of chromite layers in the upper critical zone at RPM Union Section mine, western Bushveld Complex. *In* Guidelines to the Evolution of Chromitite Ore Fields (C.W. Stowe, ed.). Hutchinson & Ross, Stroudsburg, Penn. (in press).

_____, MITCHELL, A.A. & BOTHA, M.J. (1983): Partitioning of Cr, V, Ti, Co and Ni between silicate and oxide phases within sections of the western Bushveld Complex. *National Geoscience Programme, Final Report, C.S.I.R., South Africa.*

_____ & REYNOLDS, I.M. (1983): The nature of the chromitite layers within the UG-1 – Bastard Reef interval, PRM Union Section. *Symp. on the Bushveld Complex (Pretoria), Programme with Abstr.*

FERINGA, G. (1959): The geological succession in a portion of the northwestern Bushveld (Union Section) and its interpretation. *Geol. Soc. S. Afr. Trans.* **62**, 219-233.

FLEET, M.E. (1979): Partitioning of Fe, Co, Ni and Cu between sulfide liquid and basaltic melts and the composition of Ni–Cu sulfide deposits – a discussion. *Econ. Geol.* **74**, 1517-1519.

_____ & MACRAE, N.D. (1983): Partition of Ni between olivine and sulfide and its application to Ni–Cu sulfide deposits. *Contr. Mineral. Petrology* **83**, 75-81.

_____, _____ & HERZBERG, C.T. (1977): Partition of nickel between olivine and sulfide: a test for immiscible sulfide liquids. *Contr. Mineral. Petrology* **65**, 191-197.

_____, _____ & OSBORNE, M.D. (1981): The partition of nickel between olivine, magma and immiscible sulfide liquid. *Chem. Geol.* **32**, 119-127.

HALL, A.L. (1932): The Bushveld Igneous Complex of the Central Transvaal. *Geol. Surv. S. Afr., Mem.* **28.**

HAMILTON, J.D. (1977): Sr isotope and trace element studies of the Great Dyke and Bushveld mafic phase and their relation to Early Proterozoic magma genesis in South Africa. *J. Petrology* **18**, 24-52.

HARMER, R.E. & SHARPE, M.R. (1985): Field relations and strontium isotope systematics of the Marginal rocks of the eastern Bushveld Complex. *Econ. Geol.* **80**, 813-837.

HARRIS, D.C. & NICKEL, E.H. (1972): Pentlandite compositions and associations in some mineral deposits. *Can. Mineral.* **11**, 861-878.

HART, S.R. & DAVIS, K.E. (1978): Nickel partitioning between olivine and silicate melt. *Earth Planet. Sci. Lett.* **40**, 203-219.

HATTON, C.J. & VON GRUENEWALDT, G. (1983): Magma intrusion and faulting in the development of the middle group of chromitite layers in the eastern and western Bushveld Complex. *Symp. on the Bushveld Complex (Pretoria), Programme with Abstr.*

HAUGHTON, D.R., ROEDER, P.L. & SKINNER, B.J. (1974): Solubility of sulfur in mafic magmas. *Econ. Geol.* **69**, 451-467.

HIEMSTRA, S.A. (1979): The role of collectors in the formation of the platinum deposits in the Bushveld Complex. *Can. Mineral.* **17**, 469-482.

HUPPERT, H.E. & SPARKS, R.S.J. (1980): The fluid dynamics of a basaltic magma chamber replenished by influx of hot, dense ultrabasic magma. *Contr. Mineral. Petrology* **75**, 279-289.

IRVINE, T.N. (1980): Magmatic infiltration metasomatism, double-diffusive fractional crystallization and adcumulus growth in the Muskox intrusion and other layered intrusions. *In* Physics of Magmatic Processes (R.B. Hargraves, ed.), Princeton Univ. Press, Princeton, N.J.

_____ (1982): Terminology for layered intrusions. *J. Petrology* **23**, 127-162.

_____, KEITH, D.W. & TODD, S.G. (1983): The J-M platinum-palladium reef of the Stillwater Complex, Montana. II. Origin by double-diffusive convective magma mixing and implications for the Bushveld Complex. *Econ. Geol.* **78**, 1287-1334.

_____ & SHARPE, M.R. (1983): Bushveld chilled margin liquids. II. Implications for the critical zone. *Symp. on the Bushveld Complex (Pretoria), Programme with Abstr.*

JACKSON, E.D. (1961): Primary textures and mineral associations in the Ultramafic Zone of the Stillwater Complex, Montana. *U.S. Geol. Surv. Prof. Pap.* **358**.

_____ (1970): The cyclic unit in layered intrusions – a comparison of repetitive stratigraphy in the ultramafic parts of the Stillwater, Muskox, Great Dyke and Bushveld Complexes. *In* Symp. on the Bushveld Igneous Complex and other Layered Intrusions (D.J.L. Visser & G. Von Gruenewaldt, eds.). *Geol. Soc. S. Afr. Spec. Publ.* **1**, 391-424.

KELSEY, C.H. (1965): Calculation of the CIPW norm. *Mineral. Mag.* **34**, 276-283.

KINLOCH, E.D. (1982): Regional trends in the platinum-group mineralogy of the critical zone of the Bushveld Complex, South Africa. *Econ. Geol.* **77**, 1328-1347.

KRUGER, F.J. & MARSH, J.S. (1982): The significance of $^{87}Sr/^{86}Sr$ ratios in the Merensky cyclic unit of the Bushveld Complex. *Nature* **298**, 53-55.

_____ & _____ (1985): The mineralogy, petrology, and origin of the Merensky cyclic unit in the western Bushveld Complex. *Econ. Geol.* **80**, 958-974.

LEE, C.A. (1983): Trace and platinum-group element geochemistry and the development of the Merensky unit of the western Bushveld Complex. *Mineral. Deposita* **18**, 173-190.

_____, SHARPE, M.R. & VILJOEN, E.A. (1983): The chemistry of chromitite layers in the Bushveld Complex, with special reference to chromitite–plagioclase reaction. *Symp. Bushveld Complex (Pretoria). Programme with Abstr.*

LIEBENBERG, L. (1970): The sulphides in the layered sequence of the Bushveld Igneous Complex. *In* Symp. Bushveld Igneous Complex and other Layered Intrusions (D.J.L. Visser & G. Von Gruenewaldt, eds.). *Geol. Soc. S. Afr. Spec. Publ.* **1**, 108-207.

MCBIRNEY, A.R. & NOYES, R.M. (1979): Crystallization and layering of the Skaergaard Intrusion. *J. Petrology* **20**, 487-554.

MCLAREN, C.H. & DE VILLIERS, J.P.R. (1982): The platinum-group chemistry and mineralogy of the UG-2 chromitite layer of the Bushveld Complex. *Econ. Geol.* **77**, 1348-1366.

NALDRETT, A.J. (1979): Partitioning of Fe, Co, Ni and Cu between sulfide liquid and basaltic melts and the composition of Ni–Cu sulfide deposits – a reply and further discussion. *Econ. Geol.* **74**, 1520-1528.

_____ (1981): Nickel sulfide deposits; classification, composition and genesis. *Econ. Geol. 75th Anniv. Vol.*, 628-685.

_____ & CABRI, L.J. (1976): Ultramafic and related mafic rocks: their classification and genesis with special reference to the concentration of nickel sulfides and platinum-group elements. *Econ. Geol.* **71**, 1131-1158.

_____, GASPARRINI, C., BARNES, S.J., SHARPE, M.J. & VON GRUENEWALDT, G. (1983): Cyclic units at the top of the critical zone of the Bushveld Complex and the origin of the Merensky Reef. *Symp. on the Bushveld Complex (Pretoria), Programme with Abstr.*

NORRISH, K. & HUTTON, J.T. (1969): An accurate X-ray spectrographic method for the analysis of a wide range of geological samples. *Geochim. Cosmochim. Acta* **33**, 431-453.

RAJAMANI, V. & NALDRETT, A.J. (1978): Partitioning of Fe, Co, Ni and Cu between sulfide liquid and basaltic melts and the composition of Ni–Cu sulfide deposits. *Econ. Geol.* **73**, 82-93.

RAZIN, L.V. (1976): Geological and genetic features of forsterite dunites and their platinum-group mineralization. *Econ. Geol.* **71**, 1371-1376.

ROEDER, P.L. (1974): Activity of iron and olivine solubility in basaltic liquids. *Earth Planet. Sci. Lett.* **23**, 397-410.

SHARPE, M.R. (1985): Strontium isotope evidence for preserved density stratification in the main zone of the Bushveld Complex, South Africa. *Nature* **316**, 119-126.

SHIMA, H. & NALDRETT, A.J. (1975): Solubility of sulfur in an ultramafic melt and the relevance of the system Fe–S–O. *Econ. Geol.* **70**, 960-967.

SPARKS, R.S.J. & HUPPERT, H.E. (1984): Density changes during the fractional crystallization of basal-

tic magmas: fluid dynamic implications. *Contr. Mineral. Petrology* **85**, 300-309.

THOMPSON, J.F.H., BARNES, S.J. & DUKE, J.M. (1984): The distribution of nickel and iron between olivine and magmatic sulfides in some natural assemblages. *Can. Mineral.* **22**, 55-66.

TODD, S.G., KEITH, D.W., LEROY, L.W., SCHISSEL, D.J., MANN, E.L. & IRVINE, T.N. (1982): The J-M platinum–palladium reef of the Stillwater Complex, Montana. I. Stratigraphy and petrology. *Econ. Geol.* **77**, 1454-1480.

VAN ZYL, J.P. (1970): The petrology of the Merensky Reef and the associated rocks on Swartklip 988, Rustenburg District. *In* Symp. Bushveld Igneous Complex and other Layered Intrusions (D.J.L. Visser & G. Von Gruenewaldt, eds.). *Geol. Soc. S. Afr. Spec. Publ.* **1**, 80-107.

VERMAAK, C.F. (1976): The Merensky Reef – thoughts on its environment and genesis. *Econ. Geol.* **71**, 1270-1298.

_____ & HENDRIKS, L.P. (1976): A review of the mineralogy of the Merensky Reef, with special reference to new data on the precious metal mineralogy. *Econ. Geol.* **71**, 1244-1269.

VILJOEN, M.J., DE KLERK, W.J., COETZER, P.M., HATCH, N.P., KINLOCH, E.D. & PEYERL, W. (1986a): The Union Section of Restonburg Platinum Mines Limited with reference to the Merensky Reef. *In* Mineral Deposits of Southern Africa (C.R. Anhaeusser & S. Maske, eds.). *Geol. Soc. S. Afr.*, 1061-1090.

_____, THERON, J.C., UNDERWOOD, B., WALTERS, B.M., WEAVER, J. & PEYERL, W. (1986b): The Amandelbult Section of Restonburg Platinum Mines Limited with reference to the Merensky Reef. *In* Mineral Deposits of Southern Africa (C.R. Anhaeusser & S. Maske, eds.). *Geol. Soc. S. Afr.*, 1041-1060.

VON GRUENEWALDT, G. (1979): A review of some recent concepts of the Bushveld Complex with particular reference to sulfide mineralization. *Can. Mineral.* **17**, 233-256.

WAGER, L.R. & BROWN, G.M. (1968): *Layered Igneous Rocks.* Oliver & Boyd, Edinburgh.

_____, _____ & WADSWORTH, W.J. (1960): Types of igneous cumulates. *J. Petrology* **1**, 73-85.

WAGNER, P.A. (1929): *The Platinum Deposits and Mines of South Africa.* Oliver & Boyd, Edinburgh.

WILLEMSE, J. (1969): The geology of the Bushveld Igneous Complex, the largest repository of magmatic ore deposits in the world. *In* Magmatic Ore Deposits (H.D.B. Wilson, ed.). *Econ. Geol., Mon.* **4**, 1-22.

Received October 30, 1984, revised manuscript accepted April 9, 1986.